

B. TECH. PROJECT REPORT

On

Preparation and Characterization of Copper Oxide Thin Films for CO Gas Sensing Applications

BY
RIJUL BHARAT SAGAR (160005031)



**DISCIPLINE OF METALLURGY ENGINEERING AND MATERIALS
SCIENCE**

INDIAN INSTITUTE OF TECHNOLOGY INDORE

December 2019

Preparation and Characterization of Copper Oxide Thin Films for CO Gas Sensing Applications

A PROJECT REPORT

*Submitted in partial fulfillment of the
requirements for the award of the degree*

of

BACHELOR OF TECHNOLOGY

in

METALLURGY ENGINEERING AND MATERIALS SCIENCE

Submitted by:

RIJUL BHARAT SAGAR (160005031)

Guided by:

Dr. Jayaprakash Murugesan, Assistant Professor (Internal Supervisor)

Dr. Sumanta Samal, Assistant Professor (Internal Supervisor)

Dr. M. Senthil Kumar, Principal Scientist (External Supervisor)



INDIAN INSTITUTE OF TECHNOLOGY INDORE

December 2019

CANDIDATE'S DECLARATION

I hereby declare that the project entitled “**Preparation and Characterization of Copper Oxide Thin Films for CO Gas Sensing Applications**” submitted in partial fulfillment for the award of the degree of Bachelor of Technology in ‘Metallurgy Engineering and Materials Science’ completed under the supervision of **Dr. Jayaprakash Murugesan (Assistant Professor), Dr. Sumanta Samal (Assistant Professor) in the Discipline of Metallurgy Engineering and Materials Science, IIT Indore and Dr. M. Senthil Kumar (Principal Scientist), CSIR-NPL** is an authentic work.

Further, I declare that I have not submitted this work for the award of any other degree elsewhere.

RIJUL BHARAT SAGAR

CERTIFICATE by BTP Guides

It is certified that the above statement made by the student is correct to the best of our knowledge.

(Dr. M. JAYAPRAKASH)

(Assistant Professor)

(Dr. S. SAMAL)

(Assistant Professor)

(Dr. M. SENTHIL KUMAR)

(Principal Scientist)

Preface

This report on “Preparation and Characterization of Copper Oxide Thin Films for CO Gas Sensing Applications” is prepared under the guidance of **Dr. Jayaprakash Murugesan (Internal Supervisor), Dr. Sumanta Samal (Internal Supervisor) and Dr. M. Senthil Kumar (External Supervisor).**

In this report, I have discussed about the preparation of copper thin films on glass substrate by thermal evaporation process followed by thermal oxidation to form copper oxide films. By the use of various characterization techniques, I could analyze the structural properties, surface morphology, electrical properties and CO gas sensing characteristics of copper oxide thin films.

I have tried to the best of my knowledge and ability to explain the content in a comprehensible way. I have also added figures to make the content more illustrative.

Rijul Bharat Sagar

B.Tech. IV Year

Discipline of Metallurgy Engineering and Materials Science

IIT Indore

Acknowledgements

I wish to thank my external supervisor, **Dr. M. Senthil Kumar** from CSIR-NPL for their kind support and valuable guidance. It is their help and support, due to which I was able to complete my BTP report. Without their support, this report would not have been possible.

I also would like to thank **Dr. Preetam Singh, Dr. Govind Gupta, Dr. Vishal Baloria, Ms. Debashrita Mahana, Mr. Amit Mauraya and Mr. Nitish Saini** from CSIR-NPL for their help and guidance during my research work in CSIR-NPL, New Delhi. I am highly grateful to my external supervisor and lab members for all their kind support.

I would like to thank my internal supervisors, **Dr. Jayaprakash Murugesan and Dr. Sumanta Samal** from IIT Indore for encouraging me to explore the research facilities at one of India's renowned research laboratory. I also would like to thank **Dr. Parasharam Shirage and Dr. Santosh Hosmani** from IIT Indore for giving me an opportunity to do my research work in CSIR-National Physical Laboratory, popularly known as the National Metrology Institute of India. I express my gratitude towards the IIT Indore faculty for their kind support and knowledge imparted by them.

Last but not the least, I would like to thank my parents for their moral support throughout my life. My parents always encouraged me to choose the right path in life. Without them, nothing would have been possible for me.

Rijul Bharat Sagar

B.Tech. IV Year

Discipline of Metallurgy Engineering and Materials Science

IIT Indore

Abstract

Currently, air pollution is a very serious concern worldwide as it affects the living beings and the environment due to the release of hazardous gases by industries, automobiles, waste and stubble burning, etc. In order to detect and monitor these toxic gases, metal oxide based solid-state gas sensors are being developed. In this project, different copper oxide thin films have been prepared by thermal evaporation of copper metal on glass substrate followed by thermal oxidation (annealing). Annealing of copper thin films (of 300 nm thickness) was done at 200, 300, 350 and 400 °C respectively. Various characterization techniques were used to study the different properties of the prepared copper oxide thin films. X-ray diffraction characterization was used to study the structural properties of the prepared thin films which enabled us to know about the crystal structure, lattice parameter and crystallite size of the prepared thin films. Well-crystallized single phase CuO thin films have been achieved by the oxidation of Cu films at 400 °C for a period of 2 hours. Field emission scanning electron spectroscopic technique was used to examine the surface morphology of copper oxide thin films prepared at different temperatures, which helped us to know about the surface feature, grain size and grain boundaries for the different samples. The grain structure varied with the annealing temperature of the thin film.

Current-voltage (I-V) characterization was performed to determine the electrical resistance of the CuO thin film and the I-V characteristic curve ensured that a good Ohmic contact is formed at Ag/CuO metal-semiconductor interface. Gas sensing characteristics of CuO thin films have been studied with CO as the target gas and the CuO thin film showed good gas sensing properties at a measurement temperature of 400 °C. CuO thin film showed good sensitivity, response time (in CO gas environment) and recovery time (in oxygen environment). It is noted that other phase of copper oxide such as Cu₂O did not show good sensing properties even at measurement temperature of 400 °C. For CuO thin film, a CO sensitivity of about 24 % has been obtained for a CO gas of 915 ppm concentration.

Table of Contents

CANDIDATE’S DECLARATION	i
SUPERVISOR’S CERTIFICATE	i
CSIR-NPL CERTIFICATE	iii
PREFACE	v
ACKNOWLEDGEMENTS	vi
ABSTRACT	vii
LIST OF FIGURES	xi
LIST OF TABLES	xiii
CHAPTER 1: INTRODUCTION	1
1.1 Solid-State Gas Sensors	1
1.1.1 Theory	1
1.1.2 Applications	1
1.1.3 Types	2
1.2 Thin Films	6
1.2.1 Theory	6
1.2.2 Applications	6
1.2.3 Process Steps	7
1.2.4 Preparation	8
CHAPTER 2: THERMAL EVAPORATION PROCESS	10
2.1 Introduction	10
2.2 Principle	11
2.3 Deposition Geometry	12
2.4 Components	13

2.4.1 Vacuum Pumps	13
2.4.2 Vacuum Gauges	17
2.4.3 Vacuum Valves	19
2.4.4 Thickness Monitor	22
CHAPTER 3: EXPERIMENTAL DETAILS AND CHARACTERIZATION TECHNIQUES	23
3.1 Introduction	23
3.2 Experimental Details	23
3.2.1 Preparation of Glass Substrates	23
3.2.2 Preparation of Copper Metal (Source material)	23
3.2.3 Deposition of Copper Thin Film by Thermal Evaporation	24
3.2.4 Thermal Oxidation of Copper Thin Films	25
3.3 Characterization Techniques	26
3.3.1 X-Ray Diffraction	26
3.3.2 Field Emission Scanning Electron Microscopy (FESEM)	28
3.3.3 Current-Voltage Characteristics	30
3.3.4 Gas Sensing	32
CHAPTER 4: RESULTS AND DISCUSSIONS	34
4.1 Introduction	34
4.2 Structural Analysis	34
4.2.1 Phase Analysis	35
4.2.2 Determination of Crystallite Size	35
4.2.3 Determination of Lattice Parameters	36
4.3 Surface Morphology	38

4.4 Current-Voltage Characteristics	40
4.5 Gas Sensing Analysis	41
CHAPTER 5: CONCLUSION AND SCOPE FOR FUTURE WORK	45
5.1 Conclusion	45
5.2 Scope for Future Work	45
REFERENCES	46

List of Figures

Figure 1.1: Schematic of Semiconductor Gas Sensor.

Figure 1.2: Mechanism of Semiconductor Gas Sensors for an n-type material in
(a) Oxygen Environment and (b) Reducing Gas (CO) Environment.

Figure 1.3: Schematic of Electrochemical Gas Sensor.

Figure 1.4: Schematic of Optical Gas Sensor.

Figure 1.5: Schematic of Piezoelectric Sensor.

Figure 1.6: Thin Film Process Steps.

Figure 2.1: Schematic Diagram of a Vacuum System used in PVD
process.

Figure 2.2: Schematic Diagram of Thermal Evaporation Process.

Figure 2.3: Flux Distribution by Thermal Evaporation from Point Source and
Surface Source.

Figure 2.4: Schematic Representation of Rotary Vane Pump.

Figure 2.5: Schematic Representation of four stages of a Rotary Vane
Pump.

Figure 2.6: Schematic Representation of Turbomolecular Pump.

Figure 2.7: Schematic Representation of Diffusion Pump.

Figure 2.8: Schematic of Pirani Gauge.

Figure 2.9: Schematic Representation of Penning Gauge.

Figure 2.10: Schematic Representation of Butterfly Valve.

Figure 3.1: Thermal Evaporation System used for Cu Thin Film Deposition.

Figure 3.2: Annealing Furnace used for oxidation of Cu thin films.

Figure 3.3: Schematic Diagram of X-Ray Diffraction.

Figure 3.4: Schematic Representation of FWHM.

Figure 3.5: Schematic Diagram of Field Emission Scanning Electron
Microscope.

Figure 3.6: Graphical Representation of Ohm's Law.

Figure 3.7: Ohmic Contact (a) Before contact and (b) After contact.

Figure 3.8: Sensing Response of (a) n-type semiconductor and (b) p-type
semiconductor in reducing gas (CO) environment.

Figure 4.1: XRD patterns of Cu thin films oxidized at various annealing
temperatures.

Figure 4.2: FESEM images of copper thin films oxidized at 200, 300, 350 and
400 °C.

Figure 4.3: (a) Schematic of I-V measurement circuit. (b) I-V characteristic
curve of CuO thin films measured at 200 °C.

Figure 4.4: Gas Sensing Setup used for CO Sensing Analysis.

Figure 4.5: Resistance vs. Time plot of stable-phase CuO thin film at the
measurement temperature of 375 °C.

Figure 4.6: Resistance vs. Time plot of stable-phase CuO thin film at the
measurement temperature of 400 °C.

List of Tables

Table 4.1: Values of crystallite size analyzed for different samples.

Table 4.2: Experimental values of lattice parameters (calculated by using Unit Cell software).

Table 4.3: Theoretical values of lattice parameters (referred from JCPDS data).

Table 4.4: Electrical properties of CuO thin film measured at 200 °C.

Table 4.5: Gas Sensing Parameters of CuO thin film at measurement temperature of 400 °C.

CHAPTER 1

INTRODUCTION

1.1 Solid-State Gas Sensors

1.1.1 Theory

Many industrial or domestic activities emit gases which affects the environment. These gases are the important sources of air pollution. Majority of the gases emitted as industrial waste are poisonous like carbon monoxide, nitric oxides, sulphur oxides and so on.

In order to determine the amount of harmful or poisonous gases present in the atmosphere, special devices called “*solid-state gas sensors*” are used. Solid-state gas sensors measure the concentration level of these harmful gases like (CO, NO_x, etc) in ppm (parts per million). The importance of solid-state gas sensors in science comes from their various advantages like small size, high sensitivity in identifying very low concentrations of variety of gaseous chemical species and economical [1].

The identification of volatile organic compounds which is produced from food or from domestic products has become significant in the food industry and in indoor air quality. Multisensor systems, also known as *electronic noses*, are the advanced gas sensing devices for the purpose of analyzing the harmful gases present in the ambient [1].

1.1.2 Applications

Some of the applications for gas sensors are mentioned below.

(i) Automobiles

- Car ventilation control
- Gasoline vapour detection
- Alcohol breath tests

(ii) Safety

- Fire detection
- Leak detection
- Toxic gas detection

(iii) Indoor air quality

- Air purifiers
- Ventilation control
- Cooking control

(iv) Environmental control

- Weather stations
- Pollution monitoring

(v) Food

- Food quality control
- Packaging quality control

1.1.3 Types

There are different types of solid-state gas sensors as described below.

1.1.3.1 Semiconductor Gas Sensors

Semiconductor gas sensors (SGS), also called as *chemiresistive gas sensors*, are usually based on metal oxides (like copper oxide, tin oxide, indium oxide, etc.). The electrical conductivity of a semiconductor gas sensor is based on the mechanism of transfer of charges between the target gas and metal oxide semiconductor. The schematic of semiconductor gas sensor is shown in Figure 1.1.

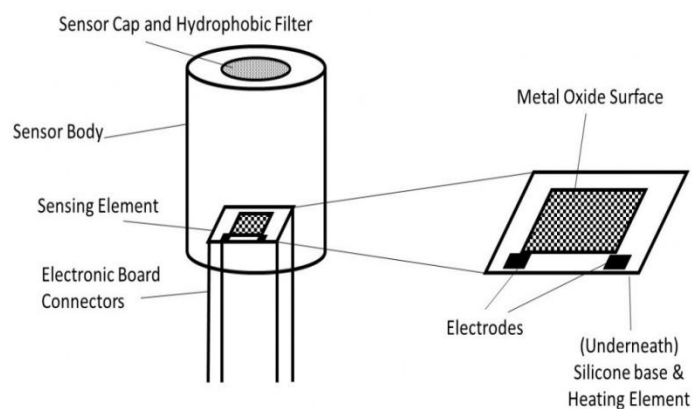


Figure 1.1: Schematic of Semiconductor Gas Sensor [2].

The gas-sensing mechanism of semiconductor gas sensors depends on the gas-semiconductor surface interactions. These surface interactions take place at the grain boundaries of the polycrystalline metal oxide thin film. The overall mechanism includes the reduction/oxidation of the semiconductor metal oxide which depends on the nature of target gas (reducing/oxidizing) which interacts with the semiconductor surface. Also, the gas-sensing mechanism depends on the adsorption of the gaseous species directly on the metal oxide semiconductor, transfer of delocalized electrons present in the conduction band to the localized states on the surface and reverse is also true. Some complex chemical reactions also occur between the different types of adsorbed gaseous species. The consequence of these surface phenomena is reversible and it causes a change in the behaviour of electrical resistance of the metal oxide thin film. This change in behaviour of electrical resistance as a function of time can be very well observed and it is used to identify the gaseous chemical species present in ambient air [1].

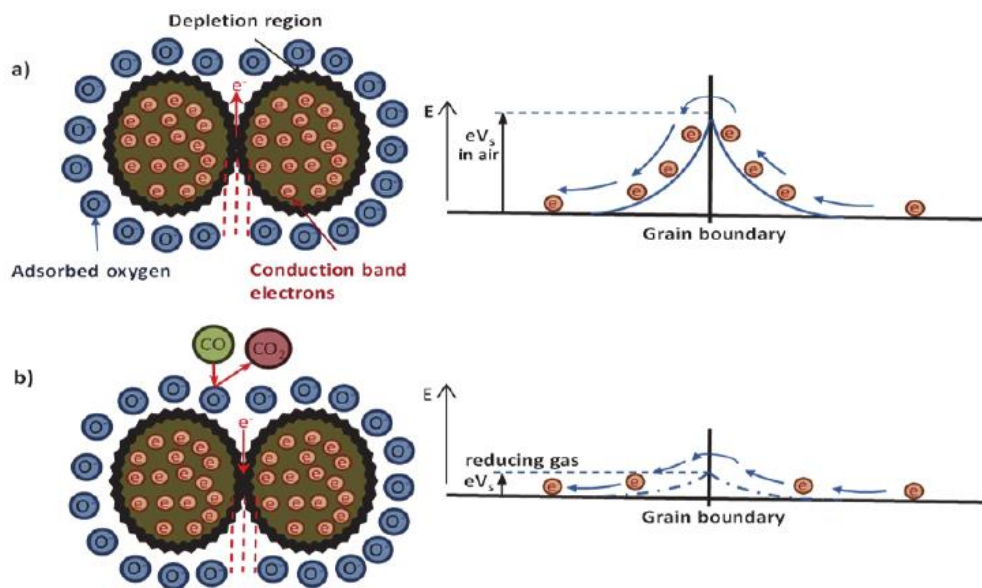


Figure 1.2: Mechanism of Semiconductor Gas Sensors for an n-type material in (a) Oxygen Environment and (b) Reducing Gas (CO) Environment [3].

Figure 1.2 describes the mechanism of semiconductor gas sensors for an n-type material (which has electrons as majority charge carriers) in reducing gas (CO) environment. Initially, in oxygen environment, the atmospheric oxygen will get adsorbed on the surface of metal oxide semiconducting material by the process of *physical adsorption* at temperatures above 200 °C. The oxygen will capture the electrons from the surface of semiconductor becoming an oxygen ion and thereby, creating an electron depletion region in metal oxide grains. So, the potential barrier for electron transport across metal oxide grains increases,

which will determine the initial resistance of the metal oxide thin film as shown in Figure 2.(a). But, in reducing gas (CO) environment, CO gas will react with the oxygen ion to emit CO₂ and the captured electrons will be released back to the metal oxide semiconductor as shown in Figure 2.(b). So, the potential barrier will decrease and thereby, decreasing the electrical resistance of n-type semiconductor as a function of time. The change of electrical resistance will be reversed for p-type semiconducting materials.

1.1.3.2 Electrochemical Gas Sensors

Electrochemical gas sensors are gas detectors that is used to measure the concentration of a target gas by reducing or oxidizing it at an electrode and measure the resultant current. These gas sensors use an electrochemical cell which consists of an envelope that contains a group of reactants which are exposed to the surroundings through two terminals, which are anode and cathode, of identical structure. The schematic of electrochemical gas sensor is shown in Figure 1.3.

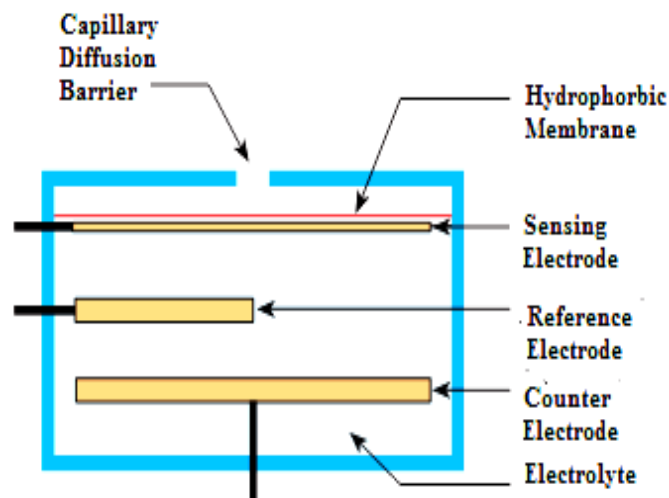


Figure 1.3: Schematic of Electrochemical Gas Sensor [4].

Electrochemical gas sensors work by the mechanism of diffusion of the target gas into the gas sensor, which generates an electric signal that is dependent on the concentration of gas. When gas interacts with the gas sensor, the gas passes through a small opening (as shown in Figure 1.3) and diffuses through a hydrophobic membrane to interact with the sensing electrode to generate enough electric signal. The diffused gas can either get oxidized at the anode or reduced at the cathode which are the end terminals of the sensing electrode. The resistor connected between the electrodes helps to determine the concentration of target gas when the current flows between the anode and the cathode.

1.1.3.3 Optical Gas Sensors

The optical gas sensors play a crucial role in field of sensing for measuring chemical and biological quantities. During the early days, the optical gas sensors were based on the changes in the absorption spectrum. Nowadays, many optical methods are employed in chemical and biosensors which includes the techniques of spectroscopy, interferometry and ellipsometry [1]. The schematic of optical gas sensors is shown in Figure 1.4. In optical gas sensors, quantity which is required can be determined by the measurement of refractive index, fluorescence and absorbance properties.

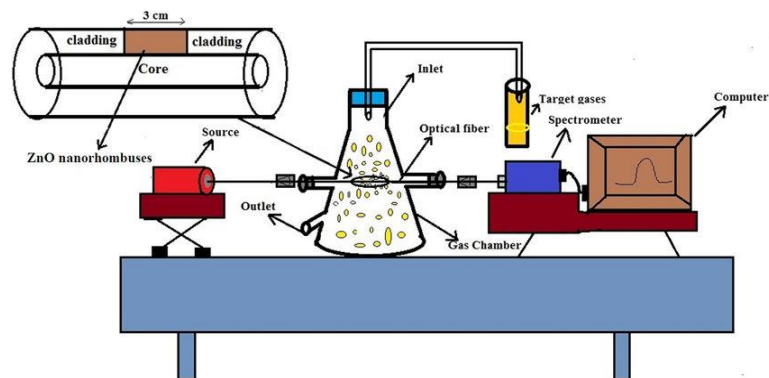


Figure 1.4: Schematic of Optical Gas Sensor [5].

1.1.3.4 Piezoelectric Sensors

It is a device that is based on piezoelectric effect, for determining the changes in acceleration, strain, pressure or force by changing them in the form of an electrical charge. The schematic of piezoelectric sensor is shown in Figure 1.5. It works based on the principle of “piezoelectric effect”. Piezoelectric effect is defined as the property of certain materials which has the tendency to generate an electrical charge in response to the applied mechanical stress [6].

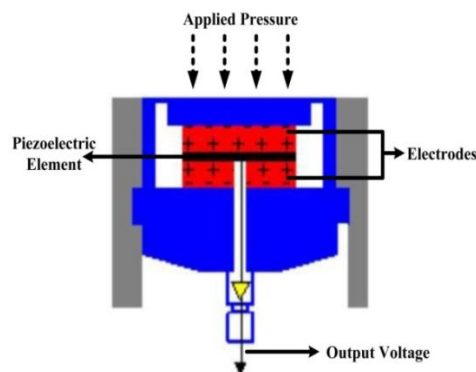


Figure 1.5: Schematic of Piezoelectric Sensor [7].

1.2 Thin Films

1.2.1 Theory

- Thin film is a two-dimensional coating of material which is restricted in one dimension.
- Substrate is a solid material which is used as a support for the thin film.
- The thickness of thinfilm is technically, 0.001 μm – 10 μm .
- For the development of solid-state gas sensors, preparation of thin films are required.
- Thin films are used for the purpose of increasing the properties at the surface of solid materials [8].
- Materials that can be deposited as thin films include: metal, dielectric, polymer, etc.

1.2.2 Applications

Some of the properties and applications of thin films are mentioned below.

(i) Optical properties

- Reflective / anti-reflective coatings.
- Compact discs.

(ii) Electrical properties

- Insulation or conduction.
- Semiconductor devices.

(iii) Magnetic properties

- Memory discs.

(iv) Chemical properties

- Shielding against corrosion.
- Gas / liquid sensors.

(v) Mechanical properties

- Hardness
- Adhesion

1.2.3 Process Steps

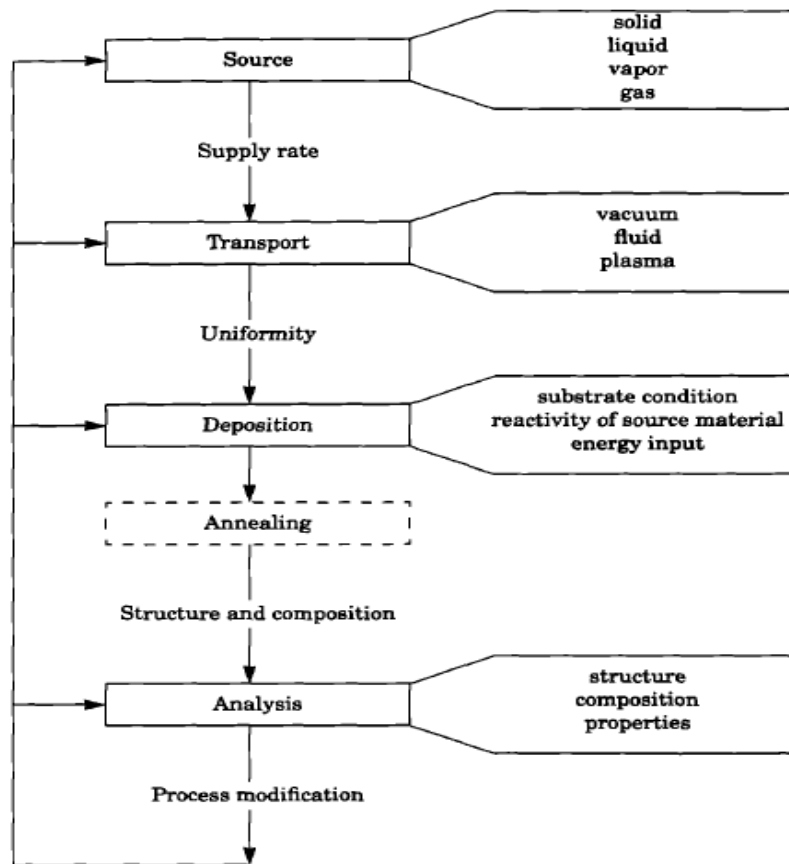


Figure 1.6: Thin Film Process Steps [9].

Figure 1.6 describes the different steps involved during a thin film deposition process. The different steps are:

- (i) Initially, a source material is required for thin film deposition. The phase of the source material can be solid, liquid, vapour or gas. The solid materials have to be vapourized in order to transport them to the surface of substrate.
- (ii) Supply rate is important because thin film properties vary with the deposition rate.
- (iii) In the transport step, the main issue lies in the uniformity of arrival rate over the surface of substrate . The factors which affect this uniformity depends on the transport medium which can be a high vacuum medium or a fluid medium.
- (iv) The next step is the deposition of thin film onto the substrate surface. There are three principal factors which determine the deposition behaviour. These factors are condition of the surface of substrate, reactivity with the target material and energy input to the substrate [9].

(v) The next step is annealing process. Annealing is mostly done to form an oxide layer of thin film on the substrate surface.

(vi) The final step is the analysis of the thin film. This step includes the various characterization techniques such as XRD and FESEM which gives us the detailed information about the structural analysis and surface morphology for the thin films respectively.

(vii) In all the steps mentioned above, process monitoring is valuable and contamination of thin film is a concern.

1.2.4 Preparation

Some of the important physical vapour deposition (PVD) techniques for the preparation of thin films are given below.

(i) *Thermal Evaporation Process:* Details about this process are explained in “Chapter 2”.

(ii) *Electron Beam Deposition:* It is a type of PVD process in which the tungsten filament is heated by the process of “thermionic emission” until it ejects electrons from its surface. The source for heating the filament is electron beam which is produced by an electron gun. Then, the electron beam is focused onto the source material (by the presence of magnets) which hits the source material and vapourises it locally. Finally, the evaporated source material gets deposited on the substrate surface to form a thin film.

(iii) *Pulsed Laser Deposition:* It is a type of PVD process in which pulsed laser beam is used as a source for heating the source material. If a solid or liquid material is exposed to a laser beam, then a small amount of material is vapourised and ejected away. Repeated pulsed laser beam produces vapour plumes (containing evaporant atoms) which will get deposited on the substrate surface to form a thin film.

(iv) *Sputtering Process:* It is a type of PVD process in which inert gas like Argon (Ar) is used. In the presence of electric field, Argon gets ionised to Ar^+ ions which hit the source material and eject atoms from it. These ions will generate plasma (hot ionised gas). With plasma as the transport medium, evaporant atoms will travel towards the substrate and finally, thin film will get deposited on the substrate surface.

(v) *Molecular Beam Epitaxy*: It is a type of PVD process in which high purity single crystal thin films can be prepared which is done in ultra high vacuum environment. Here, Knudsen cells are used as an evaporator source to vapourise the source material.

CHAPTER 2

THERMAL EVAPORATION PROCESS

2.1 Introduction

Thermal evaporation is PVD technique which is used for the synthesis of thin films. It involves heating of a source material where the material transforms from solid-liquid-vapour phase. The source for heating the material is alternating current (AC) power supply and the process of heating the source material is called “Resistive Heating” [10]. The source material to be heated is generally kept in a molybdenum (or tungsten boat) because molybdenum (tungsten) has a high melting point of 2,623 °C (3422 °C) [11] and so it can sustain a large value of current without melting.

For thermal evaporation to occur, the basic requirement is a vacuum system. The vacuum level inside the vacuum chamber is maintained in the order of 10^{-6} mbar or below before the process begins. This pressure is called the base pressure. The schematic diagram of a vacuum system is shown in Figure 2.1.

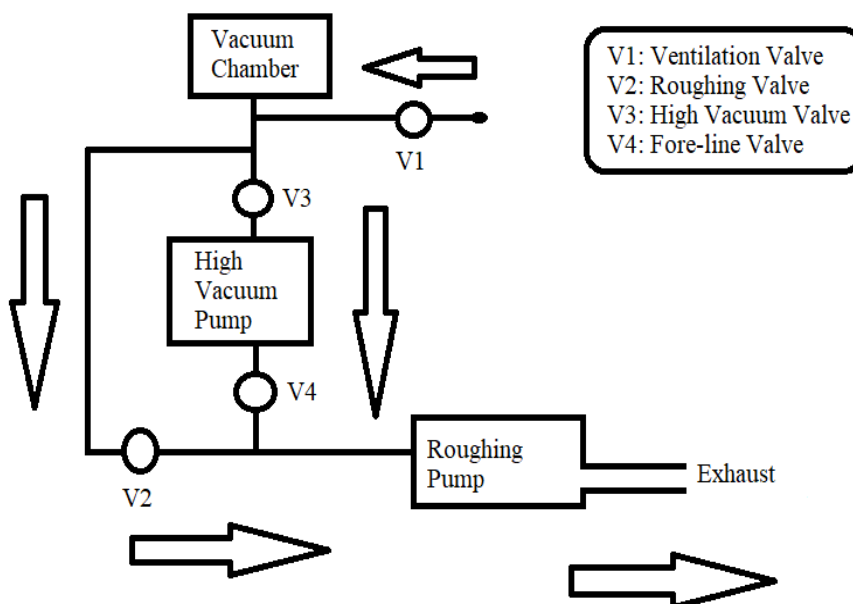


Figure 2.1: Schematic Diagram of a Vacuum System used in PVD process.

Figure 2.1 explains the different arrangements of vacuum valves, gauges and pumps in a vacuum system. When ambient air is required in the vacuum system, ‘air admittance valve’ V1 is turned on and the other valves are closed. When vacuum is required in the chamber up to pressure level of 10^{-3} Torr, V2 valve is turned on and the other valves are closed. This is called “roughing” and in this case, roughing pump removes the large gas molecules from the chamber. When vacuum is required in the chamber up to pressure level of 10^{-7} mbar, V3 and V4 valves are turned on and the other valves are closed. This is called “backing” and in this case, high vacuum pump removes the small gas molecules from the chamber and these molecules travel towards the roughing pump. When the trapped gas molecules are to be removed from the blades of turbo-molecular pump by the use of roughing pump, V4 valve is turned on and the other valves are closed. This is also called “backing”. Here, V4 valve acts as a backing valve. Whenever the roughing pump extracts the gas molecules from the chamber or high vacuum pump, these molecules are thrown out through the exhaust as shown in Figure 2.1.

High vacuum for thermal evaporation is important for two main reasons:

1. When vacuum is high, the number of gas molecules reduces to a great extent. So, the collisions between the gas molecules reduce and the mean free path of the gas particles is increased. Collisions between the gas molecules are not desirable [12] because it changes the path of the vapour (source material in vapour phase) which affects the coverage of the substrate.
2. High vacuum is required for film purity [12]. Gases present in the vacuum chamber can lead to contamination of the growing film.

2.2 Principle

The fundamental principle of thermal evaporation process is the heating of source material until its surface atoms have enough energy to move towards the substrate. The schematic of thermal evaporation process is shown in Figure 2.2. As the applied current is increased, the evaporation boat gets hotter and hotter until the pellets of the source material melt completely and evaporate. The evaporated atoms travel in straight lines inside the vacuum chamber (as shown in Figure 2.2) in long free-mean paths created by turbo-molecular pump and then deposit on the substrate. As the thermal evaporation process consumes thermal energy, it is important to keep the current flowing so that the evaporation

process is continuous. Increasing the applied current will increase the rate of thermal evaporation and vice-versa.

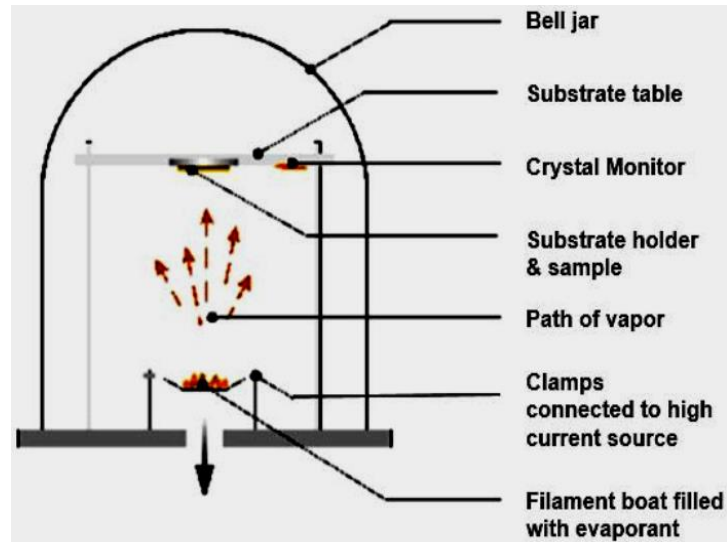


Figure 2.2: Schematic Diagram of Thermal Evaporation Process [13].

2.3 Deposition Geometry

Thin film deposition involves the consideration of both the evaporant atoms of source material and the substrate. Substrate-source material geometry influences the uniformity of thin film. Now, thermal evaporation of source material can be considered from a point source or from a surface source. Consider evaporant (vapourised source material) atoms to originate from an infinitesimally small region (dA_e) of a spherical source of surface area A_e with a uniform mass evaporation rate [14] as shown in Figure 2.3.

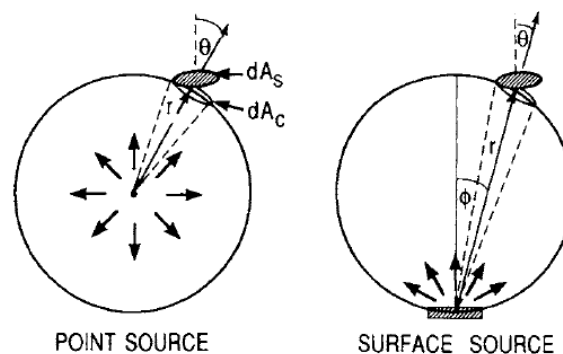


Figure 2.3: Flux Distribution by Thermal Evaporation from Point Source and Surface Source [14].

In case of evaporation from *point source*, the trajectory of evaporant atoms is “spherical”. In case of evaporation from *surface source*, the trajectory of evaporant atoms is “hemispherical”. In thermal evaporation PVD process, evaporation happens from a surface source. The total evaporated mass M_e of the source material is given by the double integral [14]:

$$\bar{M}_e = \int_0^t \int_{A_e} \Gamma_e dA_e dt. \quad \dots\dots\dots(2.1)$$

Of this amount, mass dM_s of the source material gets deposited on the substrate of area dA_s . The mass deposited per unit area for a “point source” is given by the equation [14]:

$$\frac{d\bar{M}_s}{dA_s} = \frac{\bar{M}_e \cos \theta}{4\pi r^2} \quad \dots\dots\dots(2.2)$$

The mass deposited per unit area for a “surface source” is given by the equation [15]:

$$\frac{d\bar{M}_s}{dA_s} = \frac{\bar{M}_e \cos \phi \cos \theta}{\pi r^2} \quad \dots\dots\dots(2.3)$$

With the help of the above equations, mass deposited per unit area can be determined. Also, mass of the source material deposited on the substrate surface varies directly with the deposition rate.

2.4 Components

Major components used in a thermal evaporation system are:

- Vacuum pumps
- Vacuum gauges
- Vacuum valves
- Thickness monitor

2.4.1 Vacuum Pumps

Vacuum Pumps are used to generate vacuum in the chamber at very low-pressure levels. Different types of vacuum pumps used in thermal evaporation process are described below.

(i) Rotary Vane Pump

Theory

- It falls under the category of oil-sealed positive displacement pump.
- In Ultra-High Vacuum (UHV), the major issue is the flow of oil into the vacuum chamber.
- For each revolution of the pump, a fixed volume of fluid is moved irrespective of the resistance against which the vacuum pump is pushing.
- The rotary vane pump consists of an envelope which includes gears, cams, screws and plungers operated by the rotation of the shaft.
- They can function in the pressure range of 0.5 to 10^{-2} mbar.
- For the functioning of these pumps, oil is required because it helps to provide a seal between the high-pressure and low-pressure sides of the vacuum pump and also, smoothens the pump bearings and other rotating components in the rotary vane pump.
- The schematic representation of rotary vane pump is shown in Figure 2.4.

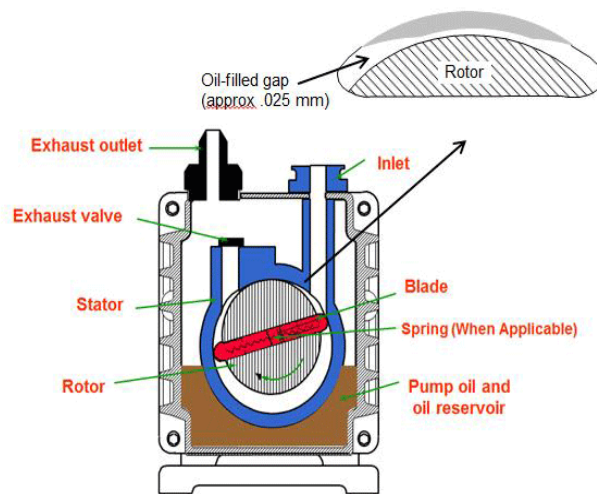


Figure 2.4: Schematic Representation of Rotary Vane Pump [15].

Working Principle of Rotary Vane Pump

There are four stages of operation in a rotary vane pump (as shown in Figure 2.5) and they are mentioned below.

- *Induction:* The 180° rotation of the rotor moves the gas into the pumping chamber. As a result, the volume which is occupied by the gas increases and the pressure which is occupied by the gas molecules decreases (Boyle's Law). So, the gas flows into the vacuum pump.
- *Isolation:* The uppermost part of vane passes the inlet port, and it seals off the inflow of gas.
- *Compression:* Further rotating of the rotor will compress and heat the incoming gas which will decrease the volume occupied by the gas and hence, the pressure occupied by the gas increases.
- *Exhaust:* As the lowermost part of vane of the rotor rotates continuously, the pressure of the gas will increase to open the exhaust valve and the incoming gas is discharged.

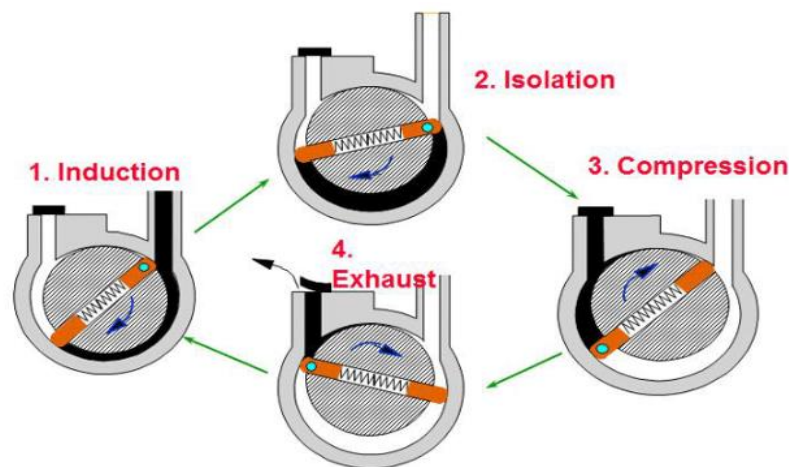


Figure 2.5: Schematic Representation of four stages of a Rotary Vane Pump [15].

(ii) Turbomolecular Pump

Theory

- It is a type of pump which is used for maintaining high vacuum level.
- This pump uses a spinning fan rotor which attacks the gas molecules.
- They can function in the pressure range of 10^{-2} to 10^{-7} mbar.
- The schematic representation of turbomolecular pump is shown in Figure 2.6.

Working Principle of Turbomolecular Pump

- Most turbomolecular pumps operate on a variety of stages, which include rotating rotor blades and stationary stator blades.

- As the gas molecules enter the chamber, these molecules will hit the rotor blades which are inclined. So, the mechanical energy will be transferred from rotor blades to the gas molecules.
- Then, the gas molecules will enter into the holes present in the stator blade.
- This will lead to the final stage where the gas molecules again hits with the surface of the rotor blades and this process is repeated, the gas molecules finally move outwards through the exhaust.

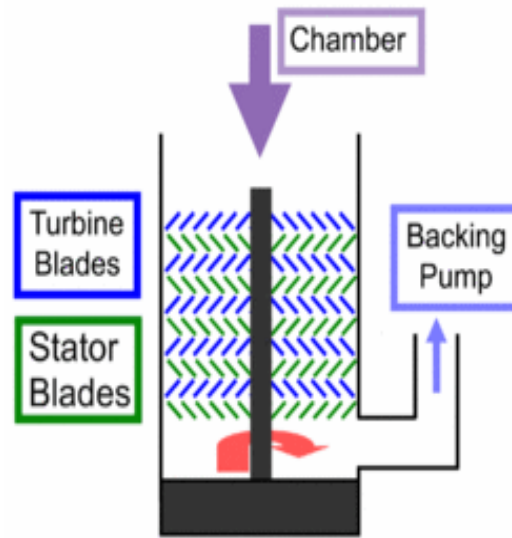


Figure 2.6: Schematic Representation of Turbomolecular Pump [16].

(iii) Diffusion Pump

Theory

- These pumps have high-speed jet of vapour to direct the flow of gas molecules in the chamber.
- It has no moving parts. Hence, they are much durable and reliable.
- It is also known as *Fluid Entrainment Pump*.
- They can function in the pressure range of 10^{-3} to 10^{-7} Torr.
- They are the most commonly used mechanisms for creating a high vacuum in industrial vacuum processing.
- The schematic representation of diffusion pump is shown in Figure 2.7.

Working Principle of Diffusion Pump

- It uses the vapour of a boiling fluid to seize the gas molecules.

- The fluid is then moved upwards because of its low density (density of hot vapours are low) and cooled by the cooling coils.
- The cooling of the vapours of boiling fluid forces the gas molecules which are captured to be released.
- Since, density increases on cooling the gas molecules and so, they travel in the downward direction.
- The gas molecules then finally reach the bottom of pump and move outwards through the exhaust.

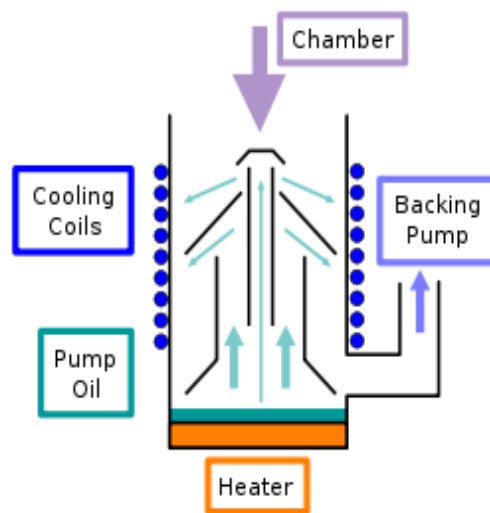


Figure 2.7: Schematic Representation of Diffusion Pump [17].

2.4.2 Vacuum Gauges

Vacuum gauges are pressure gauges used to measure the pressure levels lower than the atmospheric pressure (1 atm).

Different types of vacuum gauges used in thermal evaporation process are mentioned below.

(i) Pirani Gauge

- It is a *thermal conductivity gauge*.
- It has a metal filament kept in a tube which is connected to the vacuum system.
- This filament is attached to an electrical circuit which helps to show us the pressure reading in the vacuum chamber.
- It may be used for detecting pressure levels between 0.5 to 10^{-3} mbar.
- The schematic representation of pirani gauge is shown in Figure 2.8.

Working Principle of Pirani Gauge

- Initially, a wire (mostly platinum filament) gets heated when there is a flow of electric current through the wire.
- This wire is present in a gas and the heat is lost to the gas molecules (when the wire is heated) as the gas molecules hit the wire and extract heat.
- As the pressure of gas is lowered in the chamber by the vacuum pumps, the conductivity of the medium will decrease and the wire will lose heat at a slow pace to the gas molecules because at low-pressure levels, the number of gas molecules will decrease and so, the collision of gas molecules with the metallic wire will also reduce.
- Determining the heat loss through a wire is an indication of pressure level.

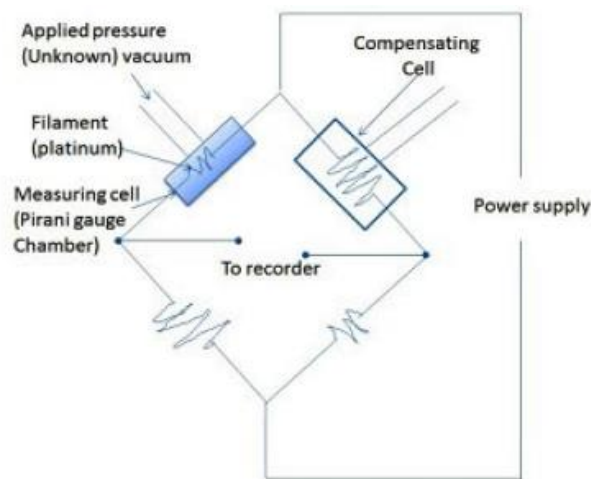


Figure 2.8: Schematic of Pirani Gauge [18].

(ii) Penning Gauge

- It is a type of cold cathode type ionisation gauge which has anode and cathode as electrodes.
- The outer cylinder is cathode which is at 25 °C and the anode is a tungsten wire.
- An externally applied voltage of 2 to 3 kV is present between anode and cathode.
- A magnetic field (produced by a permanent magnet) is also present with the electric field. This increases the ionisation current.
- It may be used for detecting pressure levels between 10^{-2} to 10^{-7} mbar.
- The schematic representation of penning gauge is shown in Figure 2.9.

Working Principle of Penning Gauge

- The electrons released from the cathode are deflected by the presence of magnetic field and the electrons move in helical path.
- The electrons will hit the gas molecules. So, the gas molecules will ionise.
- The secondary electrons are emitted by ionisation of the gas molecules.
- These secondary electrons are then seized by the anode. So, current will flow through the anode.
- The current, which is generated, determines the pressure of the gas molecules.

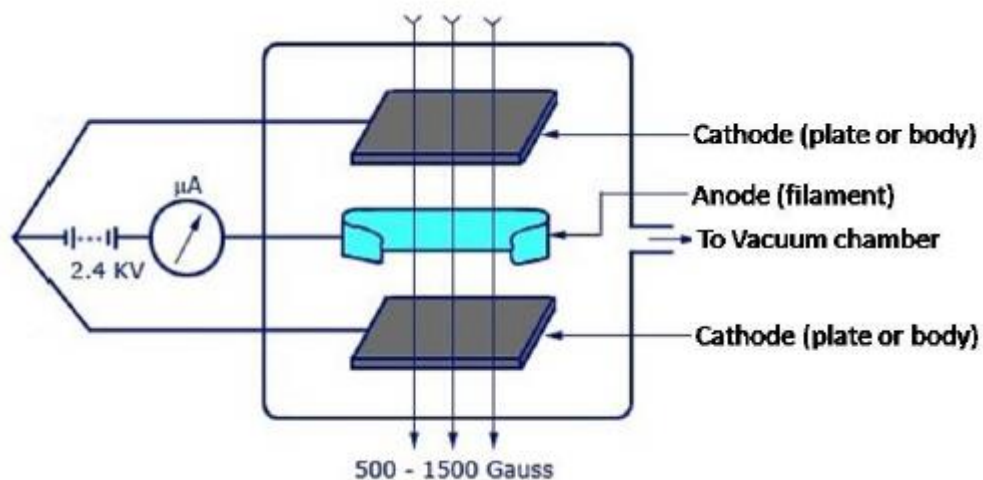


Figure 2.9: Schematic Representation of Penning Gauge [18].

2.4.3 Vacuum Valves

A vacuum valve is a device which regulates the flow of air to create a vacuum. Different types of vacuum valves used in thermal evaporation process are mentioned below.

(i) Chamber Air Admittance Valve

Theory

This valve is used for the intake of atmospheric air (present at 1 atmospheric pressure) inside the vacuum chamber so as to increase the number of gas molecules in the chamber which will increase the pressure inside the chamber and hence, the vacuum level decreases.

Working Principle of Chamber Air Admittance Valve

- The main role of “chamber air admittance valve” is to remove the vacuum created in the vacuum chamber completely.

- When this valve is opened, pressure difference is created such that the atmospheric air flows from highpressure region (atmosphere) to lowpressure region (vacuum chamber) until a complete equilibrium is established between the two regions.
- When the vacuum is to be created in the vacuum chamber, this valve must be closed so that the atmospheric air does not enter the chamber.

(ii) Combination Valve

Theory

A combination valve includes both the roughing valve and the backing valve.

Working Principle of Roughing Valve

- A roughing valve is used to connect the vacuum chamber with the rotary vane pump.
- This valve is opened when we want to remove the gas molecules from the chamber and maintain a vacuum with a pressure level of about 5×10^{-2} mbar inside the chamber.
- This valve is closed when we want to disconnect the vacuum chamber from the rotary vane pump.

Working Principle of Backing Valve

- A backing valve is used to connect the turbomolecular pump with the rotary vane pump.
- This valve is opened when we want to remove the gas molecules which are present on the blades of the turbomolecular pump and the rotary vane pump will absorb the gas molecules which are trapped in the turbomolecular pump.
- This valve is closed when we want to disconnect the turbomolecular pump from the rotary vane pump.

(iii) High Vacuum Valve

Theory

High vacuum valve, also called as “*baffle valve*” or “*butterfly valve*”, provide isolation for high vacuum pumps like turbomolecular pumps or cryogenic pumps. The schematic representation of butterfly valve is shown in Figure 2.10.

Working Principle of High Vacuum Valve

- This valve is used to connect the vacuum chamber with the turbomolecular pump.
- When this valve is opened, the turbomolecular pump will remove the gas molecules to a large extent and maintain a vacuum in the chamber with a pressure level of about 10^{-6} to 10^{-7} mbar inside the chamber.
- This valve is closed when we want to disconnect the turbomolecular pump from the vacuum chamber.

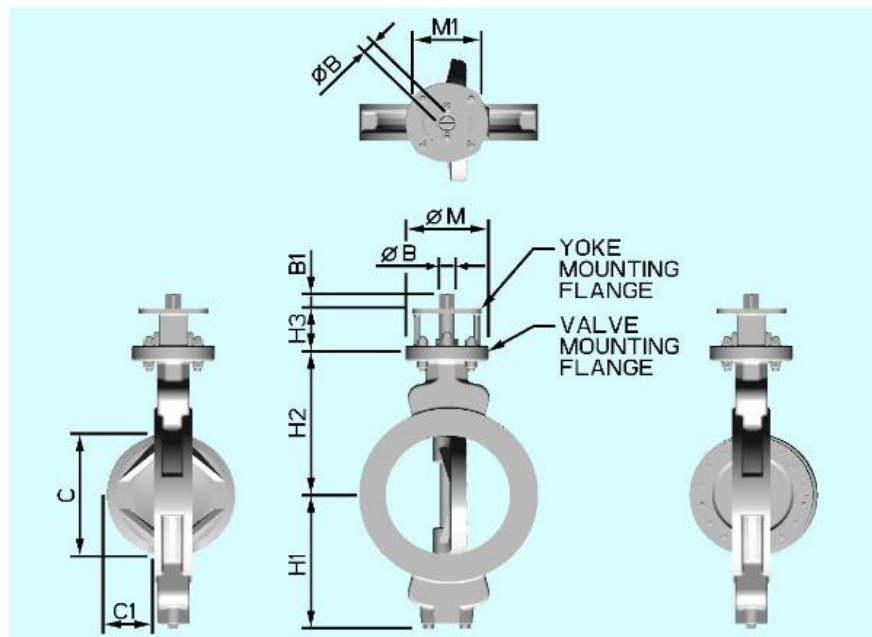


Figure 2.10: Schematic Representation of Butterfly Valve [19].

(iv) Rotary Pump Isolation Valve

Theory

This valve is used to prevent the backing of oil (present in the rotary vane pump) into the chamber during power failure and so, it acts as a *safety valve*.

Working Principle of Rotary Pump Isolation Valve

- This valve is used to provide isolation for rotary vane pump.
- This valve is opened to connect the rotary vane pump with the turbomolecular pump and the vacuum chamber.
- When we want to disconnect the rotary vane pump and isolate it completely, this valve is closed.

2.4.4 Thickness Monitor

Theory

- Deposition thickness monitor is used to measure the thickness of the film (in $\text{k}\text{\AA}$) depositing on the substrate during the deposition process.
- This instrument monitors the rate of deposition (in $\text{\AA}/\text{s}$) and it is displayed on an LED screen.
- The thickness of the film is also displayed on an LED screen.
- The thickness of the film is decided as per the requirement whereas the deposition rate can be controlled.

Working Principle of Thickness Monitor

- This instrument uses a quartz crystal as the sensor to monitor or control the film thickness.
- It is based on the principle that the film deposited on a quartz crystal can be determined by observing the change in quartz crystal's oscillating frequency.
- If the density of the target material is investigated, the thickness can be measured to a high resolution of sub-angstrom.

CHAPTER 3

EXPERIMENTAL DETAILS AND CHARACTERIZATION TECHNIQUES

3.1 Introduction

In this chapter, experimental details and various characterization techniques performed during the research work will be discussed. Experimental details include the methods adopted while doing the research work. Characterization techniques include x-ray diffraction (XRD), field emission scanning electron microscopy (FESEM), current-voltage (I-V) characteristics and CO gas sensing which were done to determine the structural analysis, surface morphology and study of electrical properties for the prepared copper oxide thin film films.

3.2 Experimental Details

3.2.1 Preparation of Glass Substrates

- Cutting of glass substrates was done by taking a glass strip and cutting it to obtain the desired dimension of 1cm x 1cm using a pencil diamond glass cutter and a scale.
- The cutting was done manually.
- Cleaning was done to remove the impurities which are present on the glass substrate.
- For cleaning of glass substrates, acetone and isopropyl alcohol were used.
- The steps for cleaning of glass substrates are listed below.
 - i. Glass substrate was dipped in acetone and sonicated for 10 minutes in sonicator.
 - ii. Now, glass substrate was dried using a dry nitrogen gun.
 - iii. Then, glass substrate was dipped in isopropyl alcohol and sonicated for 10 minutes in sonicator.
 - iv. Finally, glass substrate was dried using the dry nitrogen gun.
 - v. In all the above steps, each glass substrate was kept separately in a beaker which was first filled with acetone and then, with isopropyl alcohol.

3.2.2 Preparation of Copper Metal (Source material)

- Copper was required as a source material in thin film deposition.

- First, the copper metal was cut into small pieces to obtain the desired dimension of about 4mm x 4mm using a sheet cutter.
- Copper had some oxide layer on its periphery.
- Then, the oxide layer was removed from small copper pieces by dipping it in the mixture of hydrochloric acid and water kept in a beaker for about 10 minutes.
- Finally, the oxide layers were removed from the copper pieces which could be further used for deposition.

3.2.3 Deposition of Copper Thin Film by Thermal Evaporation

- Copper thin films were prepared by the method of “*thermal evaporation*” process. The melting point of copper is 1084 °C [11]. The thermal evaporation system used in this work is shown in Figure 3.1.
- Molybdenum boat was used as a crucible and copper as a target material. The melting point of molybdenum is 2623 °C [11]. Copper can easily melt in molybdenum boat because copper has a melting point which is less than half of the melting point of molybdenum.
- Two pieces of copper were kept in a boat.
- Before the deposition process began, the background vacuum at a pressure level of about 2.7×10^{-6} mbar (base pressure) was achieved inside the chamber. The pressure level observed during the deposition was about 1.3×10^{-5} mbar (deposition pressure).
- Also, the density and impedance values of copper were set as input in the “digital thickness monitor” in order to monitor the film thickness (in kÅ) and deposition rate.
- During the deposition process, the source material was heated by applying current using a power supply and the process of heating the source material is called as “*resistive heating*” which is defined as *the heat generated when an electric current passes through a conductor* [10]. So, in resistive heating, electrical energy is converted into heat energy.
- The applied current (in Ampere) was increased slowly in order to achieve the desired deposition rate (3.3 Å/s); a constant deposition rate (in Å/s) was maintained for the uniformity of the thin film. At an applied current of 58 A, the source material was completely evaporated.

- By achieving the desired thickness ($3 \text{ k}\text{\AA}$) as determined by the use of digital thickness monitor, the copper thin film was finally deposited on the glass substrate surface.



Figure 3.1: Thermal Evaporation System used for Cu Thin Film Deposition.

3.2.4 Thermal Oxidation of Copper Thin Films

- Annealing of copper thin films was done in a quartz tube in the presence of oxygen to form copper oxide.
- Copper oxide was further used in other applications like XRD, SEM, gas sensing, etc.
- Quartz substrate holder was used as a base material for heating the copper thin film in annealing furnace.
- The copper films were annealed in the annealing furnace (shown in Figure 3.2) at various temperatures (durations) such as $200 \text{ }^\circ\text{C}$ (5 hours), $300 \text{ }^\circ\text{C}$ (5 hours), $350 \text{ }^\circ\text{C}$ (5 hours) and $400 \text{ }^\circ\text{C}$ (2 hours) in order to study the effect of oxidation temperature on the formation of copper oxide thin films.

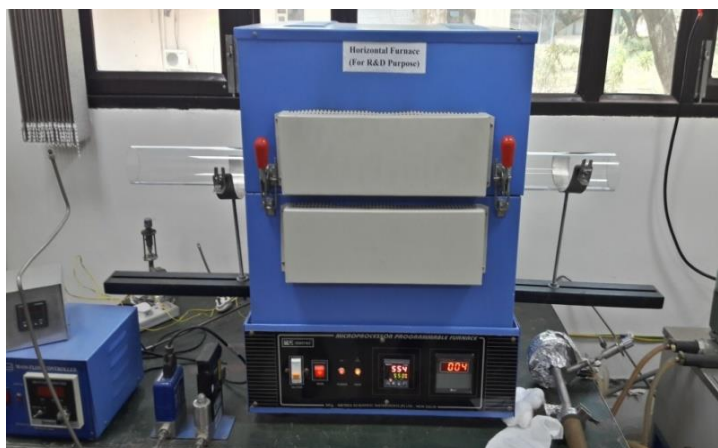


Figure 3.2: Annealing Furnace used for oxidation of Cu thin films.

3.3 Characterization Techniques

3.3.1 X-Ray Diffraction (XRD)

X-ray is a type of electromagnetic radiation with a wavelength which is shorter than the visible light. X-rays which are used in diffraction have wavelength in the range of 0.5–2.5 Å whereas visible light have wavelength in the order of 6000 Å.

X-ray diffraction is a phenomenon in which the incident X-rays are passed through a crystalline material and when these rays hit the lattice plane of the crystal, they will get diffracted at a certain angle. Since X-rays are a group of separate waves, each wave can interconnect with one another. The interaction between the waves is called interference. If the waves are in phase, then the resultant wave will have a higher amplitude which will lead to constructive interference. If the waves are out of phase, then the resultant wave will have a lower amplitude leading to destructive interference. XRD technique is used for the determination of phase, lattice parameter and crystallite size, which gives us the overall structural analysis of the crystalline material. XRD technique provides the data for intensity and 2θ values for a material. The graph obtained from XRD data shows peaks for a crystalline material and noise for an amorphous material. The schematic diagram of X-ray diffraction is shown in Figure 3.3.

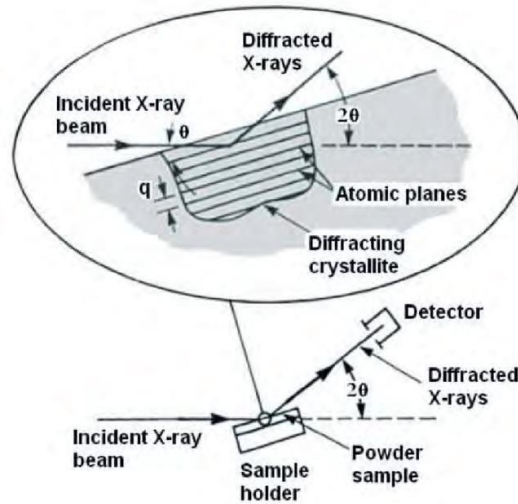


Figure 3.3: Schematic Diagram of X-Ray Diffraction [20].

XRD is based on the principle of Bragg's Law. *Bragg's Law* is given by the equation:

$$n \lambda = 2d \sin\theta \quad \dots\dots\dots(3.1)$$

where, n is the order of diffraction. (Normally, n=1 in case of XRD)

d is the interplanar spacing between two lattice planes.

θ is the angle of incidence.

λ is the X-ray wavelength of copper $K_{\alpha 1} = 1.5406 \text{ \AA}$. (Standard JCPDS data)

According to Bragg's Law, two X-ray beams with identical wavelength and phase approach towards the lattice plane of a crystalline material which will get diffracted at a certain angle θ. This will lead to interference of the waves and if constructive interference occurs, they remain in phase since the path difference between the two waves will be equal to an integer multiple of the wavelength of incident X-ray ($n\lambda$) as shown in Figure 3.3. Also, the path difference between the two waves encountering constructive interference is given by the expression of "2d sinθ". Bragg's law holds true only if constructive interference of waves occur.

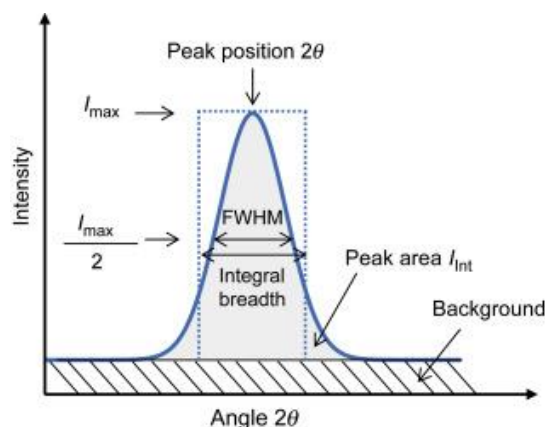


Figure 3.4: Schematic Representation of FWHM [21].

Figure 3.4 represents the schematic representation of Full-Width at Half Maximum (FWHM) which is required for determining the crystallite size. FWHM was analyzed by the use of Gauss function available in Origin software.

3.3.2 Field Emission Scanning Electron Microscopy (FESEM)

FESEM is a characterization technique which is used to study the surface morphology of the object. This technique uses an electron beam to analyze the surface microstructure of the object. These electrons are produced by a field emission source and accelerated in the presence of high electric field gradient by applying an external DC voltage of about 15 kV.

In the presence of high vacuum of about 10^{-5} Torr, the primary electrons are focussed on the object and gets deflected when it strikes the surface of the object. When the electron beam strikes the object, the valence electrons of the object are ejected as secondary electrons. These secondary electrons are detected by a detector and generates an electric signal. This signal which is generated is amplified and converted to a digital image as described in the Figure 3.5.

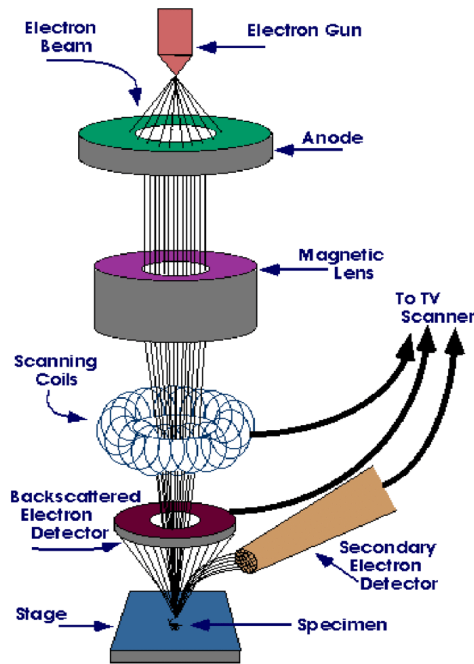


Figure 3.5: Schematic Diagram of Field Emission Scanning Electron Microscope [20].

Figure 3.5 describes the schematic of FESEM. It explains about the path of electron beam inside the high vacuum column. Electron gun is used as a source of electrons and in the presence of electric field, these electrons (being negatively charged particles) move towards the anode, which is a positively charged material. Then, these electrons are focussed in the form of electron beam by the use of electro-magnetic lenses (which includes the condenser lens and the objective lens) and the apertures in the column to a minute intense spot.

The current in the condenser is used to determine the diameter of the electron beam: a low current results in a small diameter of the beam and a high current results in a large diameter of the beam. The scanning coils are used to deflect the electron beam when they hit the object in a zig-zag pattern. The objective lens is considered as the lowest lens in the column and is used to focus the electron beam on the object.

In case of FESEM, the object must have a conductive layer for current flow. Also, high vacuum must be maintained inside the column so that the electron beam does not get deflected due to collision with the gas molecules.

3.3.3 Current-Voltage Characteristics

Current-Voltage (I-V) characteristics is the relation between current through and voltage across of electrical and electronic devices. If the I-V characteristic curve is a *straight line passing through the origin*, then it obeys Ohm's law. *Ohm's law* states that the current flowing through a conducting material at constant temperature between two points is directly proportional to the voltage or the potential difference across those two points. Ohm's law is given by the equation:

$$V = I R \quad \dots\dots\dots(3.2)$$

where, V is the potential difference across two points.

I is the current flowing the conducting material.

R is the electrical resistance of the conducting material.

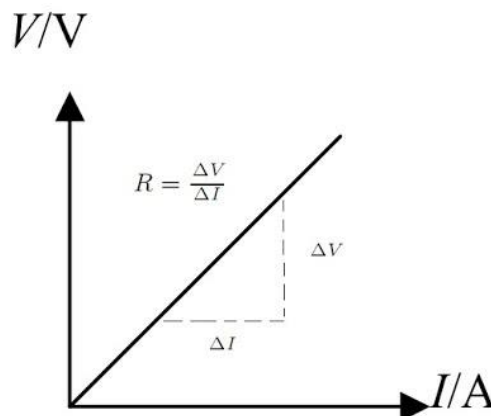


Figure 3.6: Graphical Representation of Ohm's Law [22].

Figure 3.6 shows the graphical representation of Ohm's law. The slope of the plot of current-voltage gives the value of electrical resistance of a conducting material. The electrical resistance of a conducting material is defined as the ratio of the change in potential difference with respect to the change in the current flowing through a conducting material. From Ohm's Law, $R = (V/I)$, and the slope of the I-V characteristic curve will be the inverse of the slope obtained from the graphical representation of Ohm's law (as shown in Figure 3.6) because in I-V curve, current lies on y-axis and voltage lies on x-axis. The slope of the I-V characteristic curve is given by: $(1/R) = (I/V)$.

In case of a semiconducting thin film material like copper oxide, a metallic contact is required for gas sensing applications. When a semiconductor is in contact with the metal, two types of contacts are possible: *Ohmic Contact* and *Schottky Contact*. In Schottky contact, *the work function of metal is more than the work function of semiconductor*. While in Ohmic contact, *the work function of semiconductor is more than the work function of metal* [23]. This implies that in case of Ohmic contact, it is easier to eject electrons from the semiconductor surface than from the metallic surface. In such a scenario, a low resistance contact is formed with minimal potential barrier and current can flow in both directions between the metal-semiconductor interface in Ohmic contact unlike in Schottky contact, which has a large potential barrier and current can flow in only one direction between the metal-semiconductor interface. An Ohmic contact has I-V characteristic curve as a straight line and it obeys the Ohm's law. So, for gas sensing applications, a good Ohmic contact is desirable where it is easier to study the behaviour of electrical resistance of semiconductor with time upon exposing to a target gas.

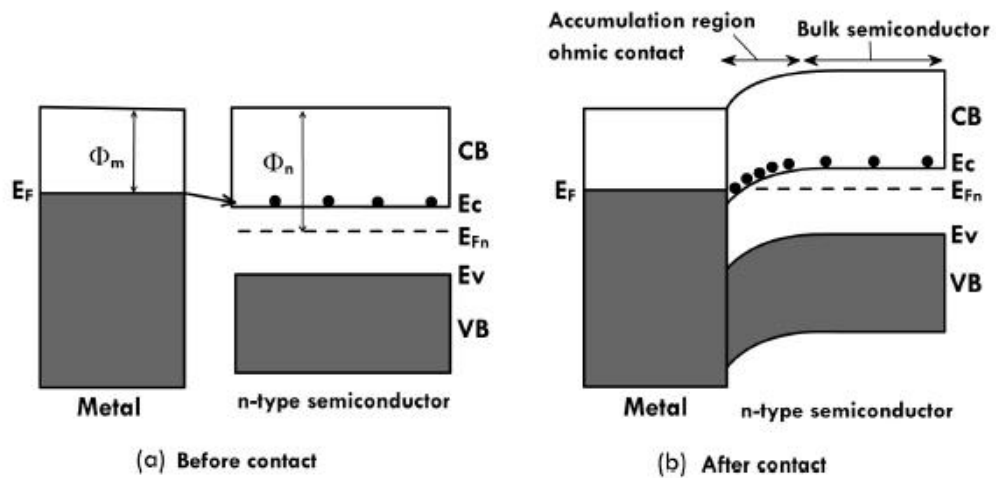


Figure 3.7: Ohmic Contact (a) Before contact and (b) After contact [23].

Figure 3.7 explains about the energy band diagram of Ohmic contact maintained at equilibrium. Before metal-semiconductor come into contact with each other, they both have different Fermi levels which leads to a difference in their work functions as shown in Figure 3.7.(a). After the metal-semiconductor come into contact with each other, at equilibrium, electrons will move from the metal (because semiconductors have high work function) to the empty states in the conduction band of the semiconductor so that the Fermi levels are aligned and thereby, an accumulation region will be formed near the interface as shown in Figure

3.7.(b). So, the interface formed will be highly conducting with minimal resistance. Thus, an Ohmic contact acts as a resistor which is conducting in both forward bias and reverse bias.

3.3.4 Gas Sensing

Gas Sensing is used to study about the electrical properties of the material which has good thermal and electrical conductivity. Gas sensing is done to detect the presence of toxic gases (like carbon monoxide, nitric oxide, etc.) present in the ambient at very low concentration levels in *parts per million* (ppm). For gas sensing applications, gas sensors are required. One of the best gas sensors used widely are *semiconductor gas sensors* because they are portable, durable, have good sensitivity and low cost.

In most of the metal oxide semiconductor gas sensors, the sensing occurs at high temperatures of about 400 °C because increase in thermal energy will lead to the flow of free electrons through the grain boundaries of metal oxide. So, oxygen can easily adsorb the free electrons from the metal oxide surface because oxygen has a high electron affinity. This will lead to the formation of potential barrier at the grain boundaries of metal oxide [24].

Some of the important parameters used in gas sensing are mentioned below.

(i) *Selectivity*: It is defined as a parameter to determine the property of a gas sensor to respond selectively to a target gas.

(ii) *Sensitivity*: It is defined as the change in measurement signal per unit concentration of the target gas. It is used to evaluate the variation of target gas concentration in the ambient.

(iii) *Response Time*: It is defined as the time required for the gas sensor to respond to a target gas to a step concentration change from zero to a certain value, that is, 90 % of the total response of the signal as shown in Figure 3.8.

(iv) *Recovery Time*: It is defined as the time required for the gas sensor to recover in oxygen environment after a step concentration change from a certain value to zero, that is, 90 % of the total recovery upon removal of the target gas as shown in Figure 3.8.

(v) *Stability*: It is defined as the ability of a gas sensor to provide almost constant results when it is continuously used for a certain period of time.

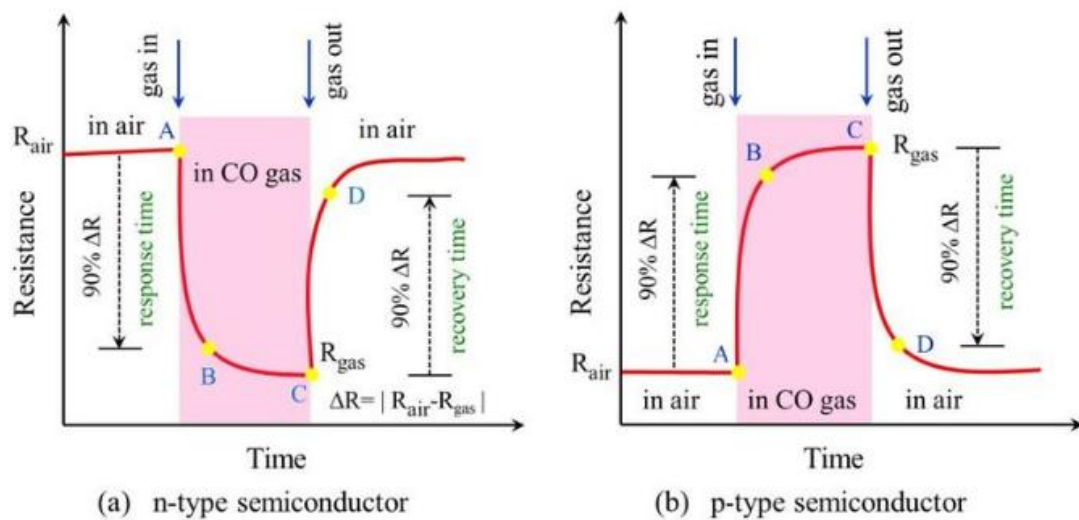


Figure 3.8: Sensing Response of (a) n-type semiconductor and (b) p-type semiconductor in reducing gas (CO) environment [25].

Figure 3.8 shows the sensing response of n-type and p-type semiconductor in CO gas environment. It explains about the behaviour of a semiconductor gas sensor in the presence of a target gas (reducing gas) at a particular temperature which shows the variation of electrical resistance of a semiconducting material with the increase in time. For example, CuO (a p-type semiconductor gas sensor) in the presence of reducing gas environment will show an increase in its electrical resistance from the original baseline to a certain value, which is considered as the response of CuO semiconductor and in the presence of oxygen environment (upon removal of reducing gas), CuO will show a decrease in its electrical resistance from a certain value obtained during its response to the original baseline as shown in Figure 3.8.(b). But, when the environment has a presence of oxidizing gas like NO_2 , the sensing response will be reversed for both n-type and p-type semiconductors.

CHAPTER 4

RESULTS AND DISCUSSIONS

4.1 Introduction

Copper oxide thin films obtained by thermal evaporation process followed by annealing at various temperature ranges (200 – 400 °C) were characterized by various techniques including XRD, FESEM, I-V Characteristics and CO Gas Sensing to analyze the structural properties, surface morphology and electrical properties. In this chapter, the properties of copper oxide thin films obtained from these characterization techniques is discussed.

4.2 Structural Analysis

X-ray diffractometer was used to analyze the structure of copper oxide thin films. XRD 2 θ -scans were done for 4 different samples of copper oxide thin films which were oxidized at various temperatures of 200, 300, 350 and 400 °C. The plots for intensity versus 2 θ are shown in Figure 4.1. From the XRD plots, it is observed that all the four samples are *polycrystalline* in nature. Also, the crystallinity of thin films increases with the increase of annealing temperature as indicated by sharp and intense XRD peaks.

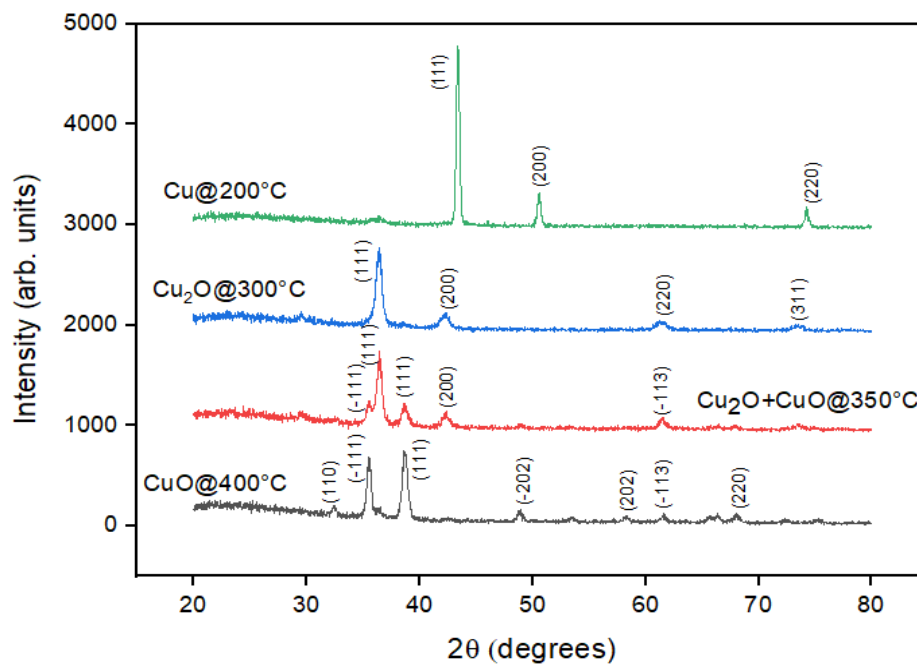


Figure 4.1: XRD patterns of Cu thin films oxidized at various annealing temperatures.

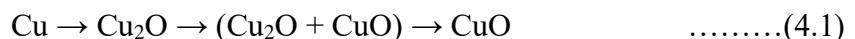
4.2.1 Phase Analysis

With the help of XRD, the phase of copper oxide samples was known by referring to JCPDS data. It is observed that on increasing the annealing temperature, the rate of oxidation is increasing and a more thermally stable phase of CuO is achieved by thermal oxidation at 400 °C.

From the XRD technique, it is noticed that copper did not get oxidized at 200 °C. As the annealing temperature is increased, the rate of diffusion of oxygen into the thin film would be much faster leading to a phase transition [26]. The increased rate of oxidation of copper oxide forms a thermally less stable phase of Cu₂O up to 300 °C; then, an intermediate phase is formed which is a mixture of Cu₂O and CuO phases when annealed at 350 °C and finally, the thermally most stable CuO phase is achieved at 400 °C.

Gibbs-Helmholtz equation says that: $\Delta G = \Delta H - T(\Delta S)$ where, Gibbs's free energy (ΔG) is determined by the change in enthalpy (ΔH), entropy (ΔS) and the absolute temperature (T). For a chemical reaction to be spontaneous, ΔG must be negative. But for temperature ranges below 300 °C, the value of ΔG is positive and so, the chemical reaction for the formation of copper oxide is non-spontaneous. But for temperature ranges above 300°C, the value of ΔG becomes negative and hence, the formation of copper oxide becomes feasible [27].

Moreover, increase in annealing temperature will enhance the diffusion kinetics of O₂ through the layer at the surface and as a result, a rapid oxidation will occur. Also, with the increase in temperature, the thermal energy will help to overcome the diffusion barrier as thermal oxidation proceeds. At the thermodynamic equilibrium, oxide phase is merely determined by the annealing temperature [27]. Therefore, it can be inferred that at equilibrium, formation of copper oxide by annealing process follows the following phase sequence:



4.2.2 Determination of Crystallite Size

The crystallite size for each sample was calculated by the use of Scherrer equation.

Scherrer equation is given by:

$$\tau = \frac{K\lambda}{\beta \cos \theta} \dots\dots\dots(4.2)$$

where:

τ is the crystallite size of the sample in nanometers.

K is the shape factor normally considered as 0.9.

θ is the Bragg's angle in degrees.

β is the full width at half maximum value of intensity (FWHM) calculated by the use of *Origin* software (β should be in radians).

λ is the X-ray wavelength of copper $K_{\alpha 1} = 1.5406 \text{ \AA}$.

For calculating the crystallite size, the values of FWHM are required. Normally, the peaks with highest intensity are preferred for this calculation. Crystallite size is calculated by using the Scherrer equation. The calculation parameters values are presented in Table 4.1.

Table 4.1: Values of crystallite size analyzed for different samples.

Sample	Lattice Plane	FWHM (in degrees)	FWHM (in radians)	2 θ (in degrees)	θ (in degrees)	cos θ	Crystallite size (in nm)
Cu	(111)	0.29219	0.005099	43.38	21.69	0.929	29.271
Cu ₂ O	(111)	0.54896	0.00958	36.38	18.19	0.95	15.235
CuO	(111)	0.46851	0.008177	38.69485	19.3474	0.9435	17.972

From Table 4.1, it is observed that the crystallite size for Cu phase was initially at a higher value of 29.271 nm, then the crystallite size reduced to a lower value of 15.235 nm for sample Cu₂O annealed at 300 °C; and finally, the crystallite size for CuO annealed at 400 °C phase was obtained as 17.972 nm. This implies that, for different phases of copper oxide which are annealed at different temperatures, the crystallite size will vary.

Compared to copper film, the crystallite size is found to lower for copper oxide films. However, the crystallite size is found to be increasing methodically with the increase in annealing temperature for copper oxide thin films [28].

4.2.3 Determination of Lattice Parameters

For calculating the lattice parameters, the value of interplanar spacing is required which can be calculated from the Bragg's Law.

Bragg's Law is given by the equation (as already discussed in Chapter 3):

$$n \lambda = 2d \sin\theta \quad \dots\dots\dots(4.3)$$

From the JCPDS file, Cu and Cu₂O belongs to *cubic* crystal system (In cubic system, a=b=c and α=β=γ=90°). CuO belongs to *monoclinic* crystal system (In monoclinic system, a≠b≠c and α=γ=90°, β≠90°).

Since, monoclinic involves four unknown lattice parameters, in order to calculate the lattice parameter values from the XRD data, the use of *Unit Cell* software was required. Whereas, cubic crystal system just involves one unknown lattice parameter and so, it can be computed manually or by the use of software. This software will give the experimental values of lattice parameters. The actual values of lattice parameters are provided in JCPDS file and so, the experimental values can be compared with the actual values of lattice parameters.

The relation between interplanar spacing and lattice parameters for cubic and monoclinic crystal system is given below [29].

Cubic:
$$\frac{1}{d^2} = \frac{h^2 + k^2 + l^2}{a^2} \quad \dots\dots\dots(4.4)$$

Monoclinic:
$$\frac{1}{d^2} = \frac{1}{\sin^2 \beta} \left(\frac{h^2}{a^2} + \frac{k^2 \sin^2 \beta}{b^2} + \frac{l^2}{c^2} - \frac{2hl \cos \beta}{ac} \right) \quad \dots\dots\dots(4.5)$$

where:

a, b and c are edge lengths or axial distances.

α, β and γ are axial angles.

The values of calculated (experimental) lattice parameters along with the actual (theoretical) values of lattice parameters are given in Tables 4.2 and 4.3.

Table 4.2: Experimental values of lattice parameters (calculated by using Unit Cell software):

Sample	Crystal System	a (in Å)	b (in Å)	c (in Å)	α (in degrees)	β (in degrees)	γ (in degrees)
Cu	Cubic	3.60929	3.60929	3.60929	90	90	90
Cu ₂ O	Cubic	4.27321	4.27321	4.27321	90	90	90
CuO	Monoclinic	4.68609	3.43232	5.12565	90	99.3805	90

Table 4.3: Theoretical values of lattice parameters (referred from JCPDS data):

Sample	Crystal System	a (in Å)	b (in Å)	c (in Å)	α (in degrees)	β (in degrees)	γ (in degrees)
Cu	Cubic	3.6150	3.6150	3.6150	90	90	90
Cu ₂ O	Cubic	4.258	4.258	4.258	90	90	90
CuO	Monoclinic	4.6893	3.4268	5.132	90	99.653	90

From the above two tables, it is observed that the experimental values of lattice parameters are in close agreement with the theoretical values. This implies that the CuO films prepared in this experiment have good crystalline quality.

4.3 Surface Morphology

Field Emission Scanning Electron Microscopy (FESEM) was used to analyze the surface morphology of copper oxide thin films which were oxidized at various temperatures such as 200, 300, 350 and 400 °C and the respective FESEM images are shown in Figure 4.2. The *magnification* of FESEM images is 1,00,000 X and a *scale* bar of 100 nm is also marked in the images.

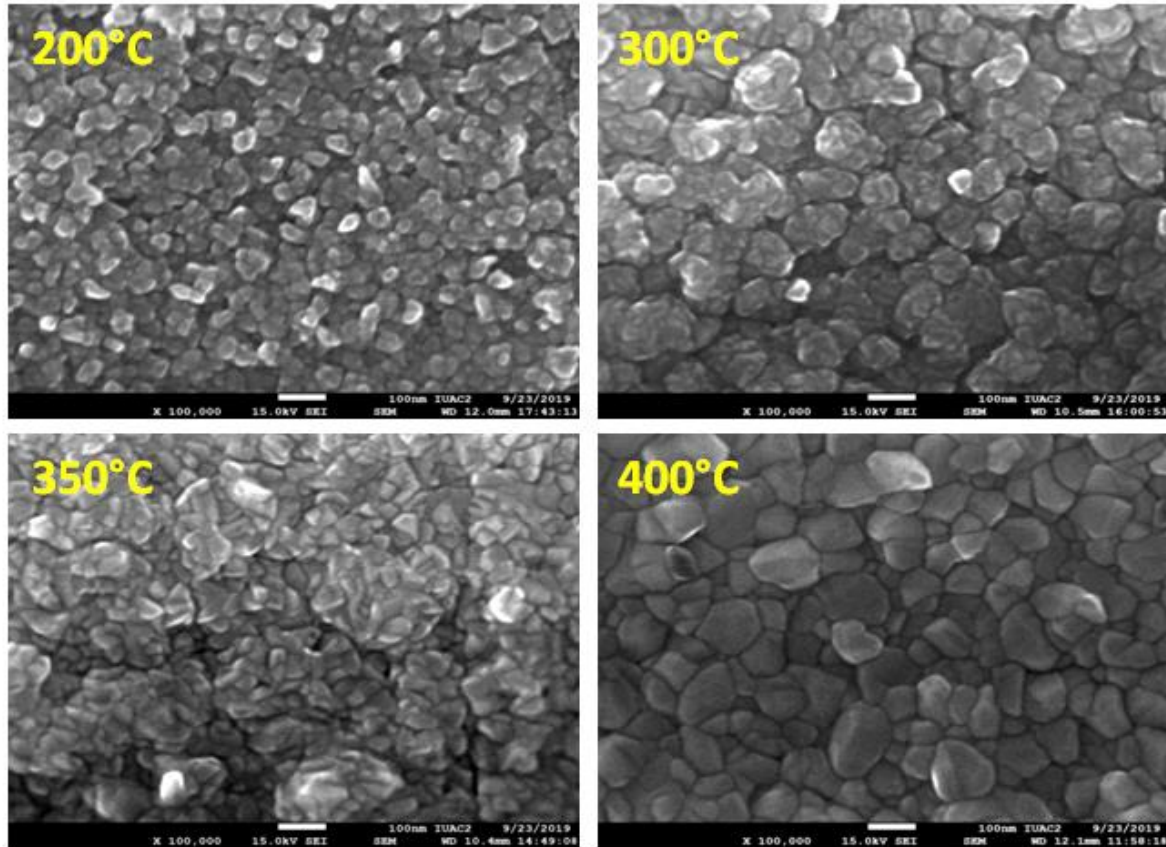


Figure 4.2: FESEM images of copper thin films oxidized at 200, 300, 350 and 400 °C.

From the above FESEM images, it is observed that the grain structure is dependent on the annealing temperature and the phase of the sample. During annealing, the following three processes occur.

1. *Recovery*: First stage of annealing cycle.
2. *Recrystallization*: Second stage of annealing cycle.
3. *Grain Growth*: Third stage or final stage of annealing cycle.

Generally, as the annealing temperature is increased, these three processes occur in a cycle, that is, first recovery occurs, then recrystallization and finally, grain growth. In the case of recovery process, annihilation and rearrangements of defects (like dislocations) occurs. However, the grain shape and grain orientation will not change. In the case of recrystallization process, formation of strain-free grains occurs. So, the grain size will increase with the increase in the recrystallization temperature. When the recrystallization process is completed (on further increasing the annealing temperature), the process of grain

growth will occur. In the case of grain growth process, the growth of strain-free grains will occur. Grain growth is accomplished by the movement of grain boundaries. So, the grain size will increase further [30].

From the FESEM images, it is analyzed that recrystallization occurs above 300 °C. At this temperature range, the formation of strain-free grains occurs. At 400 °C, it is observed that the grain size is further increasing due to the process of grain growth. Based on XRD and FESEM analyses, the stable-phase CuO thin film was considered for further characterization.

4.4 Current-Voltage Characteristics

Current-Voltage (I-V) characteristic curve ensures that the contact made between the silver paste (conducting metal) and copper oxide thin film semiconductor has a good Ohmic contact at the interface. Also, this curve helps to determine the electrical resistance (R) of copper oxide thin film by calculating the slope of I-V characteristic curve. The I-V characteristic curve of CuO thin film was measured using silver contacts as depicted in Figure 4.3(a) and the measured I-V characteristic curve is presented in Figure 4.3(b).

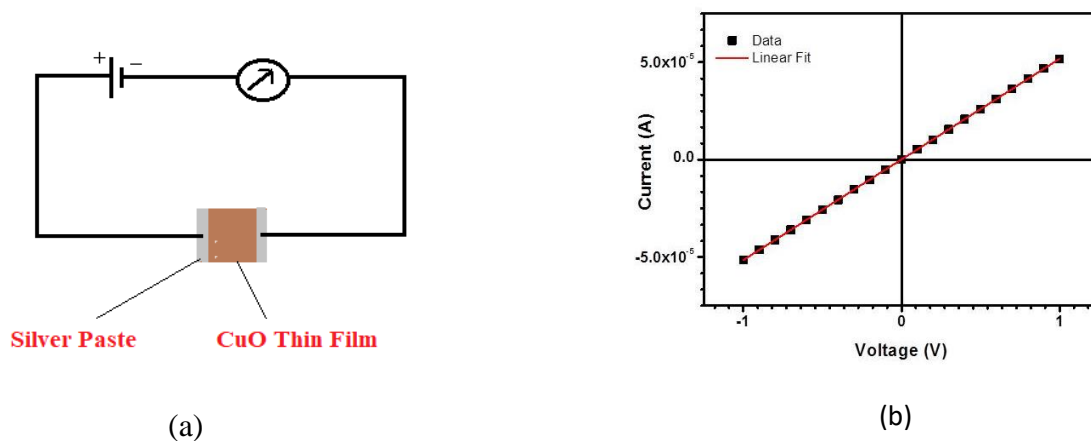


Figure 4.3: (a) Schematic of I-V measurement circuit. (b) I-V characteristic curve of CuO thin films measured at 200 °C.

From Figure 4.3, it is observed that the slope of I-V characteristic curve (gives the conductance of thin film) comes out to be $5.168 \times 10^{-5} \Omega^{-1}$ as obtained from linear fitting (using Origin software). So, the electrical resistance of CuO thin film will be 19.35 k Ω as given in Table 4.4. Also, it is observed that the contact between the silver paste and copper oxide thin film semiconductor has an Ohmic contact at the interface because the I-V characteristic curve is a straight line passing through the origin.

Table 4.4: Electrical properties of CuO thin film measured at 200 °C.

Electrical Parameters	Value
Conductance	$5.168 \times 10^{-5} \Omega^{-1}$
Resistance	19.35 k Ω

4.5 Gas Sensing Analysis

Carbon monoxide (CO) gas was used as a target gas in gas sensing analysis. CO is a reducing gas which has the tendency to donate electrons to the metal oxide semiconductor. Gas sensing was done for three different samples of copper oxide thin films annealed at 350, 375 and 400 °C in order to examine their behaviour of change in electrical resistance in the presence of oxygen and CO gas environment, one at a time.



Figure 4.4: Gas Sensing Setup used for CO Sensing Analysis.

Figure 4.4 shows the CO gas sensing setup used for gas sensing analysis. This setup includes a voltage regulator, step-down transformer, PID controller, vacuum chamber with heater and two metallic wires inside the chamber, Keithley source meter, two mass flow controllers (one for oxygen gas and the other for CO gas), rotary pump, and other arrangements. Voltage regulator is used for the purpose of regulation of voltage level and it produces a fixed output voltage that remains steady throughout for any change in input voltage (for example, to heat the heater up to 400 °C, 120 V power supply is required). Step-down transformer is used to decrease the voltage level and increase the current level. A PID

(Proportional Integral Derivative) controller is used to regulate temperature, pressure and other process variables. The material to be analyzed for gas sensing is kept on the heater by the use of silicone thermal paste. The heater consists of a heating element and a thermocouple. The two metallic wires acts as electrodes which makes metal-metal contact with the silver paste and silver paste makes metal-semiconductor contact with CuO thin film. Mass flow controller (MFC) is used to regulate the gas flow rate in the chamber where the material is loaded. The units used in MFC is litre/minute. Keithley source meter is an instrument that can precisely measure current (in micro amperes) for a fixed voltage. Rotary pump is used to remove the gas molecules present in the chamber. Ball valve is used to control the flow of gas by means of a hollow, perforated and rotating ball. A calibrated CO gas of concentration 915 ppm was used for gas sensing analysis and the calibrated CO gas cylinder was provided by gas metrology section of CSIR-NPL. For CO sensing measurement, the sample resistance (current) was continuously monitored at a constant applied bias of 2 V.

Good gas sensing properties like sensitivity, response time, etc. was shown only by the 400 °C annealed copper oxide thin film which has CuO phase (as analyzed from XRD), the most stable phase of copper oxide. But, 350 and 375 °C annealed copper oxide thin films (which has Cu₂O and Cu₂O+CuO phases of copper oxide respectively) did not show good sensing properties. So, it can be inferred that CuO is the most widely used material for scientific research including all the other phases of copper oxide with respect to gas sensing applications because CuO is the most stable phase of copper oxide whereas other phases of copper oxide like Cu₂O are unstable materials and cannot be considered as promising materials for gas sensing applications [31]. The CO sensing characteristics of CuO thin film at 375 and 400 °C are shown in Figures 4.5 and 4.6, respectively.

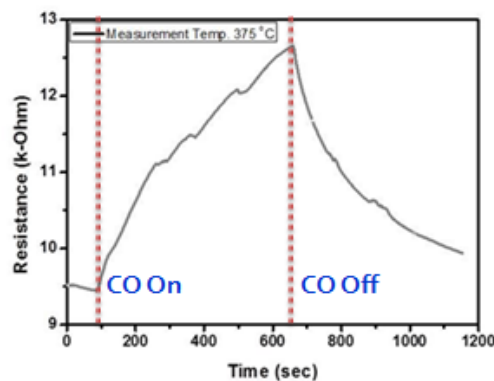


Figure 4.5: Resistance vs. Time plot of stable-phase CuO thin film at the measurement temperature of 375 °C.

From Figure 4.5, it is observed that the recovery time was not complete because the resistance of the copper oxide semiconducting film did not reach its original baseline signal from where the response of the sensing material had begun. So, at measurement temperature of 375 °C, determining the various gas sensing parameters will not provide with the accurate results. Also, it is observed that during response (in presence of CO gas), the resistance of the sensing material did not reach up to the saturation level where the resistance of the material will not be further affected by the presence of CO gas.

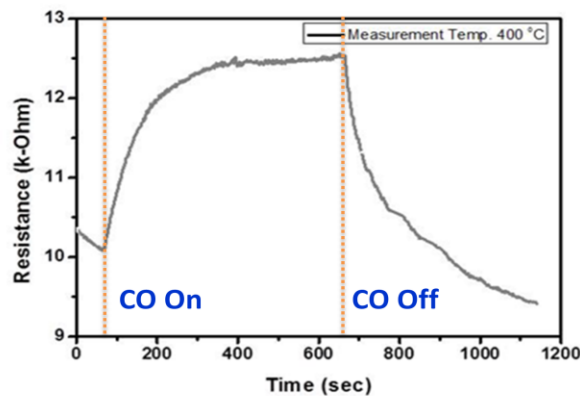


Figure 4.6: Resistance vs. Time plot of stable-phase CuO thin film at the measurement temperature of 400 °C.

A reasonably good sensing characteristics was obtained for CuO film when measured at 400 °C. From Figure 4.6, it is observed that the saturation level is reached during the response of the sensing material. Also, the recovery (in presence of oxygen environment) of the sensing material was complete where it reached the original baseline signal. Various gas sensing parameters like sensitivity, response time and recovery time are determined at from the curve. It is observed that the value of R_a is 10.1 k Ω and that of R_g is 12.48 k Ω , where, R_a is the electrical resistance of the sensing material (CuO thin film) in the presence of air and R_g is the electrical resistance of the sensing material in the presence of CO gas. The CO sensitivity is calculated by the following formula.

$$S (\%) = [(R_g - R_a) / R_a] \times 100 \quad \dots\dots\dots(4.6)$$

Response time is calculated by the time taken for 90 % increase of the change in resistance during response and the recovery time is calculated by the time taken for 90 % decrease of the total change in resistance during recovery.

Table 4.5: Gas Sensing Parameters of CuO thin film at measurement temperature of 400 °C.

Gas Sensing Parameters	Values
% Sensitivity	23.56 %
Response Time	199 s
Recovery Time	304 s

From Figure 4.6, it can be inferred that CuO is a p-type semiconductor. This is because during the response of the sensing material (in presence of reducing gas – CO gas), the electrical resistance of the material increases with time and during the recovery of the sensing material (in presence of air), the electrical resistance of the material decreases with time. This type of gas sensing mechanism is shown by p-type semiconducting material as represented by Table 4.6. This observation is complemented by the literature in which, researchers had previously reported the p-type conductivity for CuO thin films with a band gap of 1.9 – 2.1 eV [28].

Table 4.6: Variation of change in the behaviour of electrical resistance as a function of time for n-type and p-type semiconductor in the presence of reducing and oxidizing gas.

	n-type semiconductor	p-type semiconductor
Reducing gas	Decrease in resistance	Increase in resistance
Oxidizing gas	Increase in resistance	Decrease in resistance

CHAPTER 5

CONCLUSION AND SCOPE FOR FUTURE WORK

5.1 Conclusion

Copper oxide thin films were successfully prepared by the process of thermal evaporation followed by thermal oxidation (annealing). CuO, the most stable phase of copper oxide, was obtained by annealing of copper thin film at 400 °C. CuO thin film was the desired material in CO gas sensing analysis because CuO shows good gas sensing properties like sensitivity, response time and recovery time. Prior to gas sensing analysis, XRD and FESEM were used to study the structural properties and surface morphology of copper oxide thin films. XRD technique was used to determine the lattice parameters, phase analysis and crystallite size of the prepared copper oxide thin films. The crystal phase of copper oxide films is found to change with increasing oxidation temperature and more stable phases are obtained at higher oxidation temperature. Also, CuO thin film is found to be polycrystalline in nature and have a monoclinic crystal structure. With the help of FESEM technique, I could analyze the recrystallization temperature for the prepared samples where the recrystallization process began at 350 °C, and the crystal phase changed from Cu₂O to more stable CuO. I-V Characteristics was done to determine the electrical resistance of CuO thin film and to determine the Ohmic contact at the metal-semiconductor interface. In case of Ohmic contact, I-V Characteristic curve is observed to be a straight line passing through origin. From gas sensing analysis, it can be concluded that CuO is the most widely used material for research work including all other phases of copper oxide in terms of gas sensing applications. Also, for CO gas sensing, a good Ohmic contact is essential because a good Ohmic contact ensures uniform charge distribution across the semiconductor surface which is required to study the behaviour of change in electrical resistance of semiconducting material as a function of time.

5.2 Scope for Future Work

- Study of effect of thickness of film, surface morphology of film and deposition rate of film on gas sensing.
- Addition of suitable noble metals and metal-oxide based catalysts on the surface of metal oxide thin film to improve the gas sensing properties.
- Fabrication of metal oxide gas sensor devices by using suitable heaters and electrodes.

References

- [1] S. Capone, A. Forleo, L. Francioso, R. Rella, P. Siciliano, J. Spadavecchia, D. S. Presicce, A. M. Taurino: “Solid State Gas Sensors: State of the Art and Future Activities”, Journal of Optoelectronics and Advanced Materials Volume 5, 2003, Page Nos. 1335 – 1348.
- [2] <https://www.edaphic.com.au/gas-detection-encyclopedia/semiconductor-sensors/>.
- [3] Donato, Nicola & Latino, Mariangela & Neri, Giovanni. (2011). Novel carbon nanotubes-based hybrid composites for sensing applications.10.5772/18855.
- [4] Yunusa, Zainab&Hamidon, Mohd Nizar & Kaiser, Ahsanul & Awang, Z.. (2014). Gas Sensors: A Review. Sensors and Transducers. 168. 61-75.
- [5] Subramaniam, Narasimman & L., Balakrishnan & Meher, S & Rajalingam, Sivacoumar & Alex, Zachariah. (2017). Influence of surface functionalization on the gas sensing characteristics of ZnO nanorhombuses. Journal of Alloys and Compounds.706. 10.1016/j.jallcom.2017.02.160.
- [6] <https://www.nanomotion.com/piezo-ceramic-motor-technology/piezoelectric-effect/>.
- [7] Razak, Abdul & Zayegh, Aladin & Begg, Rezaul & Wahab, Yufridin. (2012). Foot Plantar Pressure Measurement System: A Review. Sensors (Basel, Switzerland). 12. 9884-912. 10.3390/s120709884.
- [8] Frey H. (2015) Applications and Developments of Thin Film Technology. In: Frey H., Khan H.R. (eds) Handbook of Thin-Film Technology. Springer, Berlin, Heidelberg.
- [9] Donald L.Smith: “Thin-Film Deposition Principles and Practice”, International Edition, Page Nos. 4 - 5.
- [10] <https://www.chegg.com/homework-help/definitions/electric-resistance-heating-4>.
- [11] <https://www.americanelements.com/meltingpoint.html>.
- [12] <https://angstromengineering.com/tech/resistive-thermal-evaporation/>.
- [13] Enam, F. & Rahman, Kazi Sajedur & Akhtaruzzaman, Md & Sopian, Kamaruzzaman & Islam, Mohammad & Amin, Nowshad. (2017). Growth of p-type CdZnTe Thin Films as

Prospective Absorber Layer for Photovoltaic Application. 10.4229/EUPVSEC20172017-3CV.1.53.

[14] <https://www.physics.byu.edu/faculty/allred/585/Ohring/Chapter%203.pdf>.

[15] <https://vacaero.com/information-resources/vacuum-pump-technology-education-and-training/195875-oil-sealed-rotary-vane-pumps.html>.

[16] https://en.wikipedia.org/wiki/Turbomolecular_pump.

[17] https://en.wikipedia.org/wiki/Diffusion_pump.

[18] https://www.iitk.ac.in/ibc/Vacuum_Gauges.pdf.

[19] <https://www.butterfly-valves.org/butterfly-valve-design/>.

[20] Billah, Areef. (2016). Investigation of multiferroic and photocatalytic properties of Li doped BiFeO₃ nanoparticles prepared by ultrasonication. 10.13140/RG.2.2.23988.76166.

[21] J. Epp,4 - X-ray diffraction (XRD) techniques for materials characterization, Editor(s): Gerhard Hübschen, Iris Altpeter, Ralf Tschuncky, Hans-Georg Herrmann, Materials Characterization Using Nondestructive Evaluation (NDE) Methods, Woodhead Publishing, 2016, Pages 81-124.

[22] <http://fizik-fizik.blogspot.com/2010/02/ohms-law.html>.

[23] <https://nptel.ac.in/content/storage2/courses/113106062/Lec9.pdf>.

[24] Chengxiang Wang, Longwei Yin, Luyuan Zhang, Dong Xiang, and RuiGao: “Metal Oxide Gas Sensors: Sensitivity and Influencing Factors”, Sensors (Basel). 2010; 10(3): 2088–2106.

[25] Santhaveesuk, Theerapong. (2015). Metal oxide semiconducting gas sensor technology (Review article in Thai). NakhonPhanom University Journal. 1. 17-29.

[26] N.A. Raship, M.Z. Sahdan, F. Adriyanto, M.F. Nurfazliana, A.S. Bakri: “Effect of Annealing Temperature on the Properties of Copper Oxide Films Prepared by Dip Coating Technique”, AIP Conference Proceedings, Volume 1788, 2017, Page No. 30121.

[27] Sumita Choudhary, J. V. N. Sarma, Surojit Pande, Soraya Ababou-Girard, Pascal Turban, Bruno Lepine, Subhashis Gangopadhyay: “Oxidation mechanism of thin Cu films: A

gateway towards the formation of single oxide phase”, AIP Advances, Volume 8, 2018, Page No. 55114.

[28] D. Santos-Cruz, S.A. Mayén-Hernández, F. de Moure-Flores, J. Campos-Álvarez, Mou Pal, J. Santos-Cruz: “CuO_x thin films by direct oxidation of Cu films deposited by physical vapour deposition”, Results in Physics, Volume 7, 2017, Page Nos. 4140 – 4144.

[29] B.D. Cullity, S.R. Stock: “Elements of X-Ray Diffraction”, Pearson New International Edition, Third Edition, Page No. 615.

[30] F.C. Campbell: “Elements of Metallurgy and Engineering Alloys”, 2008 ASM International, Page Nos. 119 – 129.

[31] ArturRydosz: “The Use of Copper Oxide Thin Films for Gas-Sensing Applications”, Coatings 2018, 8, 425.